



저작자표시-비영리-변경금지 2.0 대한민국

이용자는 아래의 조건을 따르는 경우에 한하여 자유롭게

- 이 저작물을 복제, 배포, 전송, 전시, 공연 및 방송할 수 있습니다.

다음과 같은 조건을 따라야 합니다:



저작자표시. 귀하는 원저작자를 표시하여야 합니다.



비영리. 귀하는 이 저작물을 영리 목적으로 이용할 수 없습니다.



변경금지. 귀하는 이 저작물을 개작, 변형 또는 가공할 수 없습니다.

- 귀하는, 이 저작물의 재이용이나 배포의 경우, 이 저작물에 적용된 이용허락조건을 명확하게 나타내어야 합니다.
- 저작권자로부터 별도의 허가를 받으면 이러한 조건들은 적용되지 않습니다.

저작권법에 따른 이용자의 권리는 위의 내용에 의하여 영향을 받지 않습니다.

이것은 [이용허락규약\(Legal Code\)](#)을 이해하기 쉽게 요약한 것입니다.

[Disclaimer](#)

의학석사 학위논문

Generation of chimeric antigen
receptor-inducible Treg by
targeting CD40L

CD40L를 표적으로 하는 키메라항원수용체-유도
조절 T 세포 개발에 대한 연구

2021년 8월

서울대학교 대학원

의과학과 의과학전공

장 지 윤

CD40L를 표적으로 하는
키메라항원수용체-유도 조절 T
세포 개발에 대한 연구

지도 교수 박 정 규

이 논문을 의학석사 학위논문으로 제출함
2021년 4월

서울대학교 대학원
의과학과 의과학전공
장 지 윤

장지윤의 의학석사 학위논문을 인준함
2021년 7월

위 원 장 _____

부위원장 _____

위 원 _____

ABSTRACT

Introduction: Regulatory T cells (Tregs) play a role in regulating the immune response *in vivo* and maintaining self-tolerance that does not cause an autoimmune reaction to our antigen. Recently, studies on adoptive cell transfer of Tregs into an animal model of autoimmune disease are in progress. However, since Tregs exist in a small proportion *in vivo*, it is known that the process of isolation and proliferation is difficult to apply to actual clinical practice. Therefore, in this study, I used the method to increase the number of Tregs *in vivo* by using chimeric antigen receptor (CAR). CAR-inducible Treg (iTreg) has a CD40L-specific single-chain variable fragment (scFv), thus when encountering CD40L of stimulated T cells, signals are transmitted by the intracellular domain of CAR, inducing naive T cells to differentiate into Tregs.

Methods: To confirm the expression of CAR vector, sequencing was carried out and the fluorescence of CAR-transfected in HEK293FT cell line was identified. The number of virus particles was counted by enzyme-linked immunosorbent assay (ELISA) and flow cytometry. Mouse naïve CD4⁺ T cells were isolated using the magnetic-activated cell sorting (MACS) system, and the previously produced lentivirus was transferred to the enriched naïve CD4⁺ T cells. Afterward, structural and functional aspects of the expressed CAR

were verified with markers detected by fluorescence antibody staining.

Results: The expression of CAR was checked by ZsGreen fluorescence present in pLVX-IRES-ZsGreen1 vector. The extracellular domain in which the CAR was transduced to mouse naïve CD4⁺ T cells was confirmed by the binding of the soluble CD40L protein to the scFv. In addition, after culturing with activated mouse CD3⁺ T cells, the expression level of FoxP3 and other surface markers were determined.

Conclusions: The CAR-iTreg designed in this study is to target CD40L in activated T cells. After binding to CD40L, the transduced naïve CD4⁺ CAR-T cells acquire the lineage determining transcription factor; FoxP3 and surface markers of Treg cells, giving a potential to be used as a treatment for autoimmune disease and prevention of immunological rejection in transplantation.

Keywords: inducible Treg, chimeric antigen receptor, CD40L, autoimmune disease, transplantation

Student number: 2019–20372

CONTENTS

Abstract	i
Contents.....	iii
List of tables and figures.....	iv
List of abbreviations.....	v
Introduction	1
Material and methods	9
Results	14
Discussion.....	52
Reference	56
Abstract in Korean	63

LIST OF TABLES AND FIGURES

Fig 1. A vector map of CAR	9
Fig 2. Study design of CAR-iTreg	15
Fig 3. Sequence verification of CAR construct	17
Fig 4. CAR expression in HEK293FT cell line	24
Fig 5. Production of CAR-encoding lentivirus	29
Fig 6. Calculation of CAR-encoding lentivirus particles	33
Fig 7. Extracellular expression of transduced CAR-T cells	41
Fig 8. Induction of FoxP3 expression in transduced CAR-T cells	48

LIST OF ABBREVIATIONS

Treg: regulatory T cell

IL: interleukin

FoxP3: forkhead box protein 3

TGF- β : transforming growth factor- β

CTLA-4: cytotoxic T-lymphocyte antigen-4

STAT-5: signal transducer and activator of transcription 5

SMAD: sma and mad protein

TCR: T-cell receptor

MHC: major histocompatibility complex

APC: antigen-presenting cell

DC: dendritic cell

SLE: systemic lupus erythematosus

CAR: chimeric antigen receptor

scFv: single-chain variable fragment

V_H: variable fragment of heavy chain

V_L: variable fragment of light chain

Fc: fragment of crystallizable region

IRES: internal ribosomal entry site

MCS: multi-cloning site

PCR: polymerase chain reaction

P_{CMV IE}: constitutively active human cytomegalovirus immediate
early promoter

SPF: specific–pathogen free

IACUC: Institutional Animal Care and Use Committee

HEK293FT: human epithelial kidney 293FT

DMEM: Dulbecco’s modified eagle medium

FBS: fetal bovine serum

NEM AA: non–essential amino acid

HEPES: hydroxyethyl piperazine ethane sulfonic acid

RPMI: Rosewell Park Memorial Institute

IU: international unit

Opti–MEM: Opti–minimal essential medium

PEI: polyethylenimine

FACS: fluorescence–activated cell sorting

APC: allophycocyanin

Percp–Cy5.5: peridinin–chlorophyll protein–cyanin 5.5

PE–Cy7: phycoerythrin–cyanin7

PE: phycoerythrin

APC–Cy7: allophycocyanin–cyanin 7

SD: standard deviation

ANOVA: analysis of variance

JAK: Janus kinase

BLAST: basic local alignment search tool

NCBI: National Center for Biotechnology Information

FASTA: fast adaptive shrinkage threshold algorithm

GFP: green fluorescence protein

MFI: mean fluorescence intensity

VSVG: vesicular stomatitis virus g-protein

DPBS: Dulbecco's phosphate-buffered saline

ELISA: enzyme-linked immunosorbent assay

RT-qPCR: quantitative reverse transcription-polymerase chain
reaction

TU: transduction unit

sCD40L: soluble CD40L

MOI: multiplicity of infection

FMO: fluorescence minus one

CRS: cytokine release syndrome

INTRODUCTION

1. Role and differentiation of Treg

The immune system has developed to defend the body, maintain immune homeostasis, and prevent inflammation induced by ever-evolving pathogens and environmental issues while avoiding reactivity to self-tissues. By a system of self-tolerance, self-reactive cells are eliminated since cells that carry self-reactive receptors can pose a severe threat to the immune system as they can lead to the development of autoimmunity (1). To control this dysfunction in the immune system, regulatory T cells (Tregs) function as a critical player, which is widely regarded as the primary mediator of peripheral tolerance (2). Nishizuka Y, Sakakura T *et al.* have shown that thymus originated Tregs mediate dominant self-tolerance (3). Their study showed that the adoptive transfer of thymocytes or splenocytes from adult euthymic mice to neonatal thymectomy around day 3 after birth can prohibit the ongoing autoimmune disease and later identified that those T cells are subsets of the thymus-derived $CD4^+CD25^+$ T cell population (4).

Tregs are derived originally from the thymus (tTregs), as well as peripherally (pTregs) or induced (iTregs) from naïve cells. tTregs are identified as expressing both the CD4, co-receptor of the T cell receptor, and CD25, a component of the interleukin-2 (IL-2)

receptor, along with the nuclear transcription factor forkhead box protein 3 (FoxP3) which defines Treg development and function. Moreover, recent work has described that Helios, a member of the *Ikaros* gene transcription factor family, is expressed in a subset of FoxP3⁺Tregs in both mouse and human and reported as a factor promoting resistance to autoimmunity (5).

Tregs play a crucial role in preventing autoimmunity by inhibiting proliferation and cytokine production of CD4⁺ and CD8⁺ T cells, especially activated effector T cells targeted through a receptor–ligand interaction (cell surface or soluble). Treg can secrete soluble mediators that have a suppressive function, including transforming growth factor- β (TGF- β), IL-10, adenosine, or act by direct contact via cytotoxic T lymphocyte–associated antigen-4 (CTLA-4) to suppress effector T cells (6).

In this study, I focused on the characteristics of IL-2 and TGF- β which are essential for Treg differentiation, development, maintenance, survival, and expansion (7). Consistent with the critical involvement of IL-2 signals in Treg biology, it is known that *Il2*^{-/-}, or *Il2ra*^{-/-} mice suffer from lymphoproliferative autoimmune disorders (8). Conveying the signaling pathway of IL-2, IL-2 receptor is important, which emphasizes the contribution of IL-2 for Treg development. IL-2 receptor bears three different components, each possessing diverse roles. Among them, subsequent analysis of IL-2R β dependent signal transduction pathways established that the

transcription factor signal transducer and activator of transcription 5 (STAT5) are necessary and sufficient for Treg development. STAT5 binds to the promoter of the *FoxP3* gene, which suggest that IL-2R β dependent STAT5 activation promotes Treg differentiation by regulating the expression of FoxP3 (9).

In addition, TGF- β is essential in the differentiation of both pTreg and iTregs. All TGF- β s are classified as type I and type II based on their sequence similarities. Upon ligand binding, signal is transmitted by a cytoplasmic kinase domain of type I receptors by phosphorylating receptor-regulated sma and mad proteins (SMAD), which is known as the 'SMAD signaling pathway'. Upon activation of the receptors, SMAD proteins are phosphorylated by type I receptor kinase at two carboxy-terminal serine residues and translocate into the nucleus to regulate expression. TGF- β R1 is well known for phosphorylating SMAD2, and activated TGF- β R1 is mainly known to affect FoxP3 induction in T cells (10).

TGF- β induces TCR-challenged naïve CD4⁺CD25⁻ cells to become CD25⁺FoxP3⁺Tregs (11). IL-2 can increase CD122, GITR, and CTLA-4 but with minimal expression of FoxP3 (12). However, with the help of TGF- β , it is known to enhance the ability of TCR-stimulated CD4⁺CD25⁻ cells to express FoxP3 along with markers expressed with IL-2 stimulation (13-14).

2. CD40/CD40L in autoimmune disease

Multiple signals are essential to the initiation of adaptive immune responses. The primary signal starts with the engagement of the T-cell receptor (TCR), with polypeptides originated from a protein presented by a major histocompatibility complex II (MHC II) on the surface of antigen-presenting cell (APC). Afterward, costimulatory molecules serve as fundamental factors to the functional T cell response.

Especially CD40–CD40L interactions are essential for initiating the immune response and activation of antigen-specific T cells and the maturation of T cells to perform effector functions (15).

The costimulatory receptor CD40 is a 48 kDa type I transmembrane protein. CD40 is initially characterized on B cells and expressed on dendritic cells (DCs), monocytes, platelets, macrophages, and non-hematopoietic cells such as fibroblasts epithelial, and endothelial cells (16–18).

The ligand of CD40, known as CD154 or CD40L, is a type II transmembrane protein with a variable molecular weight between 32 and 39 kDa because of post-translational modifications. CD40L is characterized by a sandwich extracellular structure composed of β -sheet, α -helix loop, and a β -sheet, which allows for the trimerization of CD40L. CD40L is expressed primarily by activated T

cells, as well as activated B cells and platelets. It possesses a soluble form reported to be expressing activities similar to the transmembrane form (19).

Interestingly, components of CD40 pathways have been expressed to be exhibiting dysregulated function and enhanced expression of CD40L in a variety of autoimmune disease states such as systemic lupus erythematosus (SLE), not only in B cells and monocytes but also circulating T cells (20). Thus, many studies have been focusing on targeting CD40L as a tool to relieve pro-inflammatory cytokine expression and T cell activation while increasing anti-inflammatory cytokine expression and inhibitory T cell costimulatory factors. For example, the administration of anti-CD40L monoclonal antibody to mice *in vivo* has been shown to inhibit both primary and secondary immune responses to type II diabetes mellitus and cardiovascular disease antigens (21). Also, in primates, treatment with antibodies aiming CD40L has proven to be successful in clinical trials enabling the prolonged acceptance of allogeneic kidney transplants (22), providing a promising treatment in contributing to allograft rejection in clinical settings.

3. Chimeric antigen receptor (CAR)

CAR-based immunotherapy has been an attractive and potential therapy in treating cancer. CAR-T cell therapy uses patient-derived leukocytes, especially T cells, and modifies them to attack tumors. The first step in the production of CAR-T cells is the isolation of T cells from human blood. CAR-T cells may be manufactured either from the patient's blood, known as an autologous treatment, or from a healthy donor's blood, called an allogeneic treatment. T cells are typically treated with the cytokine IL-2 and anti-CD3, anti-CD28 antibodies to proliferate the cells extensively, then later purified and transduced with lentivirus that embraces engineered CAR (23).

What makes CAR unique is its structural feature which is a hybrid of many different domains that redirects T cells toward cells or tissues expressing the antigen of interest and empowers them to recognize antigens in an MHC-independent manner (24).

CAR, in general, consists of three major domains—ectodomain, a transmembrane domain, and endodomain. Ectodomain is a membrane protein domain outside the cytoplasm, consisting of a single-chain variable fragment (scFv) and a spacer. scFv serves as a signal peptide of ectodomain in CAR structure, arranged with a variable fragment of heavy (V_H) and light chain (V_L) chains of monoclonal antibody and fused with a linker. Spacer, also known as a hinge domain, provides a bridge-like connection between the

transmembrane and antigen-binding domains. The spacer gives a diverse movement of the binding domain to mediate antigen recognition. Proteins used in the hinge region of CAR-T cells can be the fragment crystallizable region (Fc region), the tail region of an antibody, IgG1, IgG4, IgD, and, cell surface molecules such as CD28, CD8 α , CD7 (25).

The transmembrane domain, which consists of a hydrophobic alpha helix that spans the membrane, connects the extracellular and intracellular sections of a CAR molecule. This domain is also known to influence the expression and stability of CARs (26).

Endodomain includes a costimulatory domain and CD3 ζ , which serves as the most functional end of the receptor. After antigen recognition and the help from the costimulatory domain, the receptors cluster and signal transmit to T cells, giving an initial start sign to CAR-T cells (27).

In order to escalate the activity and persistence of CAR, researchers developed the various generation by adding costimulatory domains. For example, the second generation of CAR, which contains one costimulatory domain (CD28 or 4-1BB or OX-40) is known to have enhanced activity and persistency whereas third-generation CAR which includes two or more costimulatory domains which can have tonic signaling regulating CAR-T cell performance (28-29).

As CARs have a pivotal role in controlling infectious disease

and cancer, many researchers are considering how CAR-T cell therapy could provide the solution to diseases outside the field of cancer. The most notorious CAR designed in autoimmunity and transplantation is alloantigen-specific human Tregs created with an HLA-A2 specific CAR (A2-CAR) in a peptide-independent manner, which is utilized to prevent xenogeneic graft-versus-host diseases in the immune-deficient NOD.SCID. $\gamma c^{-/-}$ mice receiving HLA-A2⁺ human PBMCs alone or with A2-CAR-expressing Tregs (30–31). Even though it showed great potential in *in vivo* experiments, isolating a lot of Tregs from splenocytes was their difficulty since Tregs only consist of a small portion in lymphocytes.

In order to obtain and utilize more abundant cells, this study focused on naïve CD4⁺ T cells and with the use of CAR to turn their lineage into iTreg cells.

MATERIALS AND METHODS

CAR Vector design

pLVX–internal ribosome entry site (IRES)–ZsGreen1 lentiviral vector (Takara bio, Mountain View, CA, USA) was used as a backbone, which has IRES between the Zsgreen1 fluorescence gene and multi-cloning site (MCS). CAR construct was obtained by over-extension polymerase chain reaction (PCR) and synthesized into a lentiviral vector (Fig. 1 A).

A

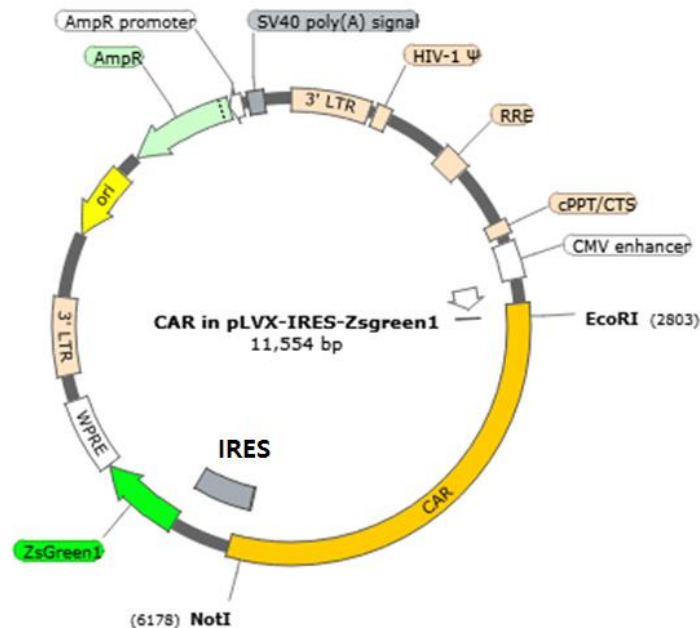


Figure 1. A vector map of CAR (A) pLVX–IRES–ZsGreen1 lentiviral vector is HIV–1 based, a lentiviral expression vector that allows the simultaneous expression of a protein of interest, in this study, CAR.

The vector expresses the two proteins from a bicistronic mRNA transcript, allowing Zsgreen to be used as an indicator of CAR. Promotion of the bicistronic transcript is driven by the constitutively active human cytomegalovirus immediate early promoter ($P_{CMV\ IE}$) located upstream of MCS. The vector map was drawn using Snapgene software (Insightful Science, San Diego, CA, USA).

Mice

C57BL/6, called the B6, were obtained from Koatech (Pyeongtaek, Korea) and housed under a specific pathogen-free (SPF) animal facility at Seoul National University. Mice were maintained by the guidelines of the Institutional Animal Care and Use Committee (IACUC Approval no. SNU-201102-2-1) and used for all experiments during week 8 to 10.

Cell lines

Human embryonic kidney 293FT (HEK293FT) cell line was purchased from Invitrogen (Carlsbad, CA, USA) and maintained in Dulbecco Modified Eagle Medium (DMEM) with high glucose (Hyclone, Logan, UH, USA) supplemented with 10% fetal bovine serum (FBS; GWvitek, Seoul, Korea) and L-glutamate, sodium pyruvate, non-essential amino acid (NEM AA), hydroxyethyl piperazine ethane sulfonic acid (HEPES), $1\times$ antibiotic-antimycotic (complete media, all from Gibco, Grand Island, NY, USA) in a

humidified incubator containing 5% CO₂ at 37° C. Until day 10, HEK293FT cells were treated with 500 µg/mL geneticin (Gibco) to maintain clones that stably express the SV40 large T antigen from the Pcmvsport6Tag. Neo plasmid (32). To enhance the transfection efficiency, HEK293FT cell line was used only until passage 15.

Primary mouse T cell isolation and culture

Naive CD4⁺ T cells were sorted from the spleen of B6 mice by negative selection using a naive CD4⁺ T cell isolation kit (Miltenyi biotec, Bergisch Galdbach, Germany). Sorted Naive CD4⁺ T cells were seeded with 1×10^5 cells in 96 U-bottom plate with media consisting of Rosewell Park Memorial Institute 1640 (RPMI 1640; Hyclone), 10% heat-inactivated FBS (GWvitek), L-glutamate, sodium pyruvate, HEPES, and NEM AA (T cell media, all from Gibco) and supplemented with 20 international unit (IU)/mL of IL-2 otherwise stated.

Transfection

Day before transfection, HEK293FT cell line (2×10^5 cells/mL) was placed in a 6-well tissue culture plate. Following day, two 1.5 mL e-tubes were prepared and labeled as A and B tubes. In A tube, 2 µg of CAR plasmid was prepared and diluted in a pre-warmed 100 µL Opti-minimal essential medium (Opti-MEM, Gibco) and B tube 8 µL of polyethyleneimine (PEI, Sigma-Aldrich, St. Louis, MO, USA)

diluted in 100 μ L Opti-MEM. Reagent in A was slowly added to B tube drop by drop and incubated at room temperature for 15 min and PEI-DNA complex was added to the culture media. Fugene HD transfection reagent (Promega, Madison, WI, USA) and DNA were prepared in a ratio of 4 (μ L): 1 (μ g) and added in 200 μ L of Opti-MEM. Fugene HD transfection reagent-DNA complex was also treated in a separate culture media. The plate was incubated in the 5% CO₂, 37° C humidified incubator for 3 days and utilized for analysis.

Flow cytometry

Fixable viability dye 660 (eBioscience, San Diego, CA, USA) and BD horizon fixable viability stain 700 (BD Biosciences, Franklin Lakes, NJ, USA) were stained to detect live cells only otherwise mentioned. Every cell used in the experiments was harvested, rinsed with 1 \times PBS, centrifuged at 500g, 5 min and re-suspended in 1 \times PBS. Dye was treated in re-suspended 1 \times PBS at a ratio of 1:1,000, vortexed immediately, and stored in 4° C, dark for 30 min.

All cells were stained with purified anti-mouse CD16/32 antibody (BioLegend, San Diego, CA, USA) for 10 min at 4° C in dark. Sorted out naive CD4⁺ T cells were washed once with 1 \times fluorescence-activated cell sorting (FACS) buffer and stained with anti-CD45 (30-F11; Allophycocyanin, APC), anti-CD3 (17A2; Brilliant Violet 421, BV421), anti-CD4 (RM4-5; Peridinin-Chlorophyll protein-

cyanine 5.5. Percp-Cy 5.5), anti-CD25 (PC61.5; Phycoerythrin-cyanine7, PE-Cy7), anti-CD62L (MEL-14; Phcoerythrin, PE), anti-CD44 (IM7; Allophycocyanin-cyanine7, APC-Cy7) antibodies for checking purity. Also sorted CD3⁺ T cells were stained with anti-CD45 (30-F11; Percp), anti-CD3 (17A2; APC-Cy7) antibodies for confirming purity. All the antibodies were purchased from BioLegend. To detect CAR-iTregs' binding to soluble CD40L (sCD40L), anti-DYKDDDDK antibody (FLAG, L5; APC, BioLegend) was stained. Also, to detect CAR-iTreg's surface and activation marker, anti-CD25 (PC61.5; Percp-Cy5.5) antibody was stained. Intracellular staining was processed using anti-FoxP3 (FJK-16s; APC and PE, eBioscience) and anti-CTLA-4 (UC10-4F10-11; PE) antibody with FoxP3 transcription factor staining buffer set (eBioscience) according to the manufacturer's recommendation. All dyes used were stained at 4° C, 1 hr in dark. All data were acquired by FACS LSR II (BD Biosciences) and evaluated using Flowjo software (Tree Star, Ashland, OR, USA).

Statistical analysis

All statistical analyses were performed using Graphpad Prism version 8 (GraphPad Software, San Diego, CA, USA). Data were shown as the mean \pm standard deviation (SD). For multiple comparisons between groups, two-tailed student's *t*-test and analysis of variance (ANOVA) with Tukey honesty significant difference test were applied.

RESULTS

1. Scheme of CAR-iTreg

A novel concept of using CAR as a tool to derive naïve CD4⁺ T cells to iTreg was designed to suggest a potential therapeutic to the unclearly defined field of autoimmunity and transplantation. To facilitate the differentiation of naïve cells to Tregs, *Il2rb* and *Tgfbr1* domains were added to the second-generation CAR construct, with scFv synthesized to target stimulated T cells to function as *in vivo* iTregs when they encounter them (Fig. 2A).

In detail, a full-length cytoplasmic domain of *Il2rb* was inserted owing to its function in increasing antigen-binding affinity and producing a docking site for Janus kinase (JAK), resulting in phosphorylation of STAT5 (33). A full-length cytoplasmic domain of *Tgfbr1* was also added, considering its function in inducing the expression of FoxP3 by phosphorylating SMADs. It is known that the combination of IL-2 with TGF- β also affects the downregulation of IL-6 receptor expression and IL-6 signaling, inhibiting the conversion to Th17 cells while promoting Treg differentiation (33).

As a whole, CAR was composed of an integrated molecule of TCR signaling domain *Cd247*, an intra-signal domain of *Il2rb*, and *Tgfbr1*, costimulatory domain *Cd28*, and scFv targeting CD40L.

A

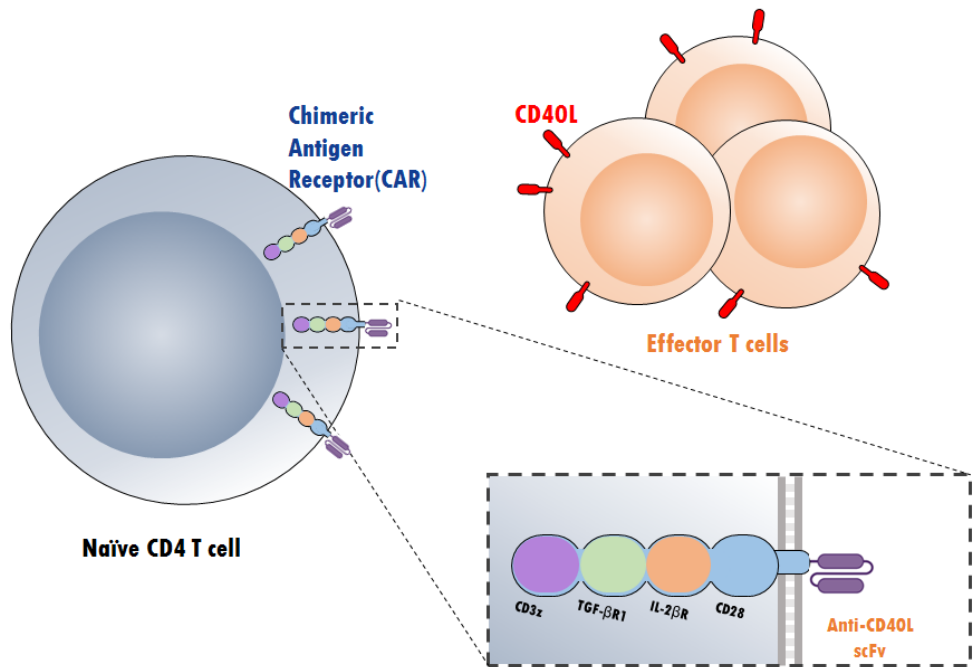


Figure 2. Study design of CAR-iTreg (A) This study is conducted to convert naïve $CD4^{+}$ CAR-T cells into iTregs when they recognize a specific antigen, CD40L.

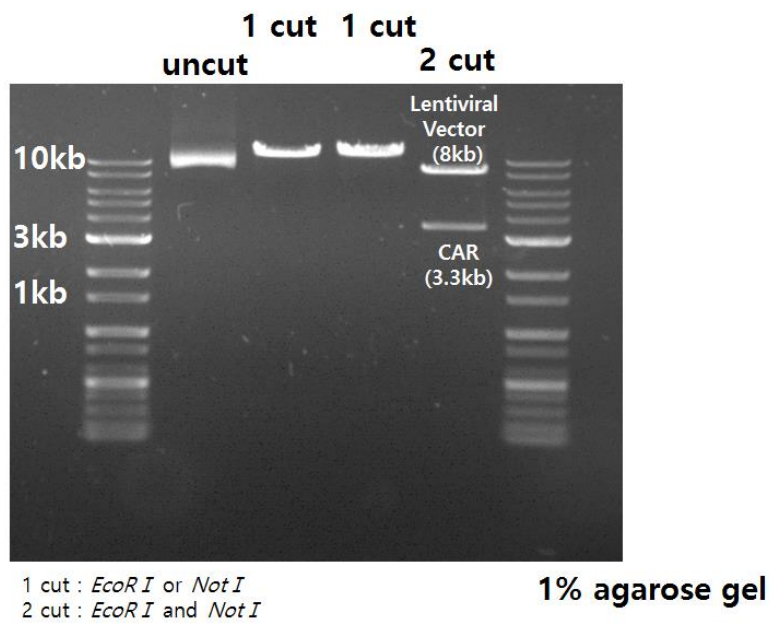
2. Confirmation of CAR sequence

1) Vector sequence verification

CAR size is estimated to range 3.5 kb, and lentiviral vector, 8 kb (Fig. 1A). To indirectly confirm the size of CAR, an endonuclease (*EcoR I*, *Not I*) cut was done which is positioned at the border of the CAR gene, respectively, in a 37° C water bath for 1 hr. The samples were loaded in the 1% agarose gel with 6× DNA sample buffer (Biofact, Daejeon, Korea), and electrophoresis was carried out at 100 V for 30 min. As expected, 2 cut lanes (*EcoR I*, *Not I*) showed 2 bands, each representing the exact size of the lentiviral vector and insert (CAR) (Fig. 3A).

DNA sequencing was done by Cosmogenetech (Seoul, Korea), provided with the primer of each independent CAR domain. The sequence was re-verified by using basic local alignment search tool (BLAST) supplied by the National Center for Biotechnology Information (NCBI). The sequence of the ectodomain (left: V_H and right: V_L) was from anti-mouse CD40L monoclonal antibody-producing hybridoma, MR1 (34), and shown in Fig. 3B. All the following query sequences originated from NCBI coding sequence fast adaptive shrinkage threshold algorithm (FASTA) (Fig. 3B).

A



B Anti-CD40L V_H sequence

Leader 1
 M N S G L Q L V F F V L T L K G I Q G E V Q
 ATGAAGCTCAGGACTCCAAATGCTTTCTTTGTCCTCACTCTAAAAGGTATACAGGGTCAGCTCCAG
 10 20
 L V E S G G G L V Q P G K S L K L S C E A S
 CTGGTGGAGTCTGGGGGAGGCTTGGTGCAGCCTGGAAAGTCCTGAAACTCTCCTGTGAGGCTCT
 30 CDR1 40
 G F T F S G Y G M H W V R Q A P G R G L E S
 GGATTCACCTTCAGCGGCTATGGCATGCACTGGGTCCGCCAGGCTCCAGGGAGGGGGCTGGAGTCG
 50 52 a CDR2 60
 V A Y I T S S S I N I K Y A D A V K G R F T
 GTCGCATACATTACTAGTAGTAGTATTAAATATCAAAATAGCTGACGCTGTGAAAGGCCGTTCCACC
 70 80 82 a b c
 V S R D N A K N L L F L Q M N I L K S E D T
 GTCTCCAGAGACAATGCCAAGAAGTACTGTTTCTACAAATGAACATTCTCAAGTCTGAGGACACA
 90 CDR3 100
 A M Y Y C A R F D W D K N Y W G Q G T M V T
 GCCATGTACTACTGTGCAAGATTCGACTGGGACAAAATTACTGGGCCCAAGGAACCATGGTCACC
 JH4
 110
 V S S
 GTCTCTCA

Score	Expect	Identities	Gaps	Strand
676 bits(366)	0.0	366/366(100%)	0/366(0%)	Plus/Plus
Query 1	CAGGTCCAGTTGAAGCAGTCTGGGGCTGAGTTTGTGAAGCCTGGAGCCTCAGTGAAGATA	60		
Sbjct 1	CAGGTCCAGTTGAAGCAGTCTGGGGCTGAGTTTGTGAAGCCTGGAGCCTCAGTGAAGATA	60		
Query 61	TCCTGCAAACTTCAGGCTATACCTTCACTGATGGCTACATGAAGTGGGTTGAGCAGAAG	120		
Sbjct 61	TCCTGCAAACTTCAGGCTATACCTTCACTGATGGCTACATGAAGTGGGTTGAGCAGAAG	120		
Query 121	CCTGGGCAGGGCCTTGAGTGGATTGGAAGAATTGATCCTGATAGTGGTGATACTAGGTAC	180		
Sbjct 121	CCTGGGCAGGGCCTTGAGTGGATTGGAAGAATTGATCCTGATAGTGGTGATACTAGGTAC	180		
Query 181	AATCAGAAGTTCAGGGCAAGGCCACACTGACTAGAGACAAATCCTCCAGCACAGTCTAC	240		
Sbjct 181	AATCAGAAGTTCAGGGCAAGGCCACACTGACTAGAGACAAATCCTCCAGCACAGTCTAC	240		
Query 241	ATGGACCTCAGGAGTCTGACATCTGAGGACTCTGCTGTCTATTACTGTGCGAGAGCCCCT	300		
Sbjct 241	ATGGACCTCAGGAGTCTGACATCTGAGGACTCTGCTGTCTATTACTGTGCGAGAGCCCCT	300		
Query 301	TATATAGCGGATATAGGGGAGGCCTTTGATTACTGGGGCCAAGGAACCATGGTCACCGTC	360		
Sbjct 301	TATATAGCGGATATAGGGGAGGCCTTTGATTACTGGGGCCAAGGAACCATGGTCACCGTC	360		
Query 361	TCCTCA	366		
Sbjct 361	TCCTCA	366		

Anti-CD40L V_L sequence

Leader 1
 M R A P T V Y P V L L F L W F T G A I C D I
 ATGAGGGCCCTACTGTGTATCCTGTGCTCTTGTTCCTTGGTTTACAGGTGCCATATGTGACATC
 10 20
 Q M T Q S P S S L P A S L G D R V T I N C Q
 CAGATGACCCAGTCTCCATCATCACTGCCTGCCTCCCTGGGAGACAGAGTCACATATCAATTGTCAG
 CDR1 30 40
 A S Q D I S N Y L N W Y Q Q K P G K A P K L
 GCCAGTCAGGACATTAGCAATTATTTAAACTGGTACCAGCAGAAACCAGGAAAGCTCCTAAGCTC
 50 CDR2 60
 L I Y Y T N K L A D G V P S R F S G S G S G
 CTGATCTATTATACAAATAAANTGGCAGATGGAGTCCCATCAAGGTTCACTGGCACTGGTTCTGGG
 70 80 90
 R D S S F T I S S L E S E D I G S Y Y C Q Q
 JAGATTCTCTTTCACTATCAGCAGCCTGGAATCCGAAGATATTGGATCTTATTACTGTCAACAG
 CDR3 100
 Y Y N Y P W T F G P G T K L E I K
 TATTATACTATCCGTGGACGTTGGACCTGGCACCAAGCTGGAAATCAA
 "JK1"

Score	Expect	Identities	Gaps	Strand
616 bits(333)	0.0	333/333(100%)	0/333(0%)	Plus/Plus
Query 1	GATATCGTGTGACACAGTCTCCATCTTCCTTGGCTGTGTCCGAGGAGACAAGGTCACC	60		
Sbjct 1	GATATCGTGTGACACAGTCTCCATCTTCCTTGGCTGTGTCCGAGGAGACAAGGTCACC	60		
Query 61	ATCAACTGCAAGTCCAGTCAGAGTCTTTTATCTGGTGGCTATACTACTTGGCTTGGTAC	120		
Sbjct 61	ATCAACTGCAAGTCCAGTCAGAGTCTTTTATCTGGTGGCTATACTACTTGGCTTGGTAC	120		
Query 121	CAGCAGAAAAACAGGGCAGTCTCCTAAATTACTGATCTATTTACATCCACTCGGCACACT	180		
Sbjct 121	CAGCAGAAAAACAGGGCAGTCTCCTAAATTACTGATCTATTTACATCCACTCGGCACACT	180		
Query 181	GGTGTCCCTGATCGCTTCATAGGCAGTGGGTCTGGGACAGATTTCACTCTAACCATCAAC	240		
Sbjct 181	GGTGTCCCTGATCGCTTCATAGGCAGTGGGTCTGGGACAGATTTCACTCTAACCATCAAC	240		
Query 241	AGTTTCCAGACTGAGGATCTGGGAGATTACTATTGTCAGCATCATTACGGTACTCCTCTC	300		
Sbjct 241	AGTTTCCAGACTGAGGATCTGGGAGATTACTATTGTCAGCATCATTACGGTACTCCTCTC	300		
Query 301	ACGTTCCGGTGATGGCACCAAGCTGGAGATAAAA	333		
Sbjct 301	ACGTTCCGGTGATGGCACCAAGCTGGAGATAAAA	333		

Cd28 transmembrane sequence

Score	Expect	Identities	Gaps	Strand
582 bits(315)	5e-162	315/315(100%)	0/315(0%)	Plus/Plus
Query 1	AAAATTGAGTTCATGTACCTCCGCCTTACCTAGACAACGAGAGGAGCAATGGAAC TATT	60		
Sbjct 518	AAAATTGAGTTCATGTACCTCCGCCTTACCTAGACAACGAGAGGAGCAATGGAAC TATT	577		
Query 61	ATTCACATAAAAGAGAAACATCTTTGTCATACTCAGTCATCTCCTAAGCTGTTTTGGGCA	120		
Sbjct 578	ATTCACATAAAAGAGAAACATCTTTGTCATACTCAGTCATCTCCTAAGCTGTTTTGGGCA	637		
Query 121	CTGGTCGTGGTTGCTGGAGTCCTGTTTGTATGGCTTGCTAGTGACAGTGGCTCTTTGT	180		
Sbjct 638	CTGGTCGTGGTTGCTGGAGTCCTGTTTGTATGGCTTGCTAGTGACAGTGGCTCTTTGT	697		
Query 181	GTTATCTGGACAAATAGTAGAAGGAACAGACTCCTTCAAAGTGACTACATGAACATGACT	240		
Sbjct 698	GTTATCTGGACAAATAGTAGAAGGAACAGACTCCTTCAAAGTGACTACATGAACATGACT	757		
Query 241	CCCCGGAGGCCCTGGGCTCACTCGAAAGCCTTACCAGCCCTACGCCCTGCCAGAGACTTT	300		
Sbjct 758	CCCCGGAGGCCCTGGGCTCACTCGAAAGCCTTACCAGCCCTACGCCCTGCCAGAGACTTT	817		
Query 301	GCAGCGTACCGCCCC	315		
Sbjct 818	GCAGCGTACCGCCCC	832		

Il2rb cytoplasmic domain sequence

Score	Expect	Identities	Gaps	Strand
1502 bits(813)	0.0	813/813(100%)	0/813(0%)	Plus/Plus
Query 1	AAGTGCCGGTACCTTGGGCCATGGCTGAAGACAGTTCTCAAGTGCCACATCCCAGATCCT	60		
Sbjct 894	AAGTGCCGGTACCTTGGGCCATGGCTGAAGACAGTTCTCAAGTGCCACATCCCAGATCCT	953		
Query 61	TCTGAGTTCTTCTCCAGCTGAGCTCCAGCATGGGGGAGACCTTCAGAAATGGCTCTCC	120		
Sbjct 954	TCTGAGTTCTTCTCCAGCTGAGCTCCAGCATGGGGGAGACCTTCAGAAATGGCTCTCC	1013		
Query 121	TCGCCTGTCCCTTGTCTTCTTCAGCCCCAGTGGCCCTGCCCTGAGATCTCTCCGCTG	180		
Sbjct 1014	TCGCCTGTCCCTTGTCTTCTTCAGCCCCAGTGGCCCTGCCCTGAGATCTCTCCGCTG	1073		
Query 181	GAAGTGCTCGACGGAGATTCCAAGGCCGTGCAGCTGCTCCTGTTACAGAAGGACTCTGCC	240		
Sbjct 1074	GAAGTGCTCGACGGAGATTCCAAGGCCGTGCAGCTGCTCCTGTTACAGAAGGACTCTGCC	1133		
Query 241	CCTTTACCTCGCCAGCGGCCACTCACAGGCCAGCTGCTTACCAACCAGGGCTACTTC	300		
Sbjct 1134	CCTTTACCTCGCCAGCGGCCACTCACAGGCCAGCTGCTTACCAACCAGGGCTACTTC	1193		
Query 301	TTCTTCCATCTGCCCAATGCCTTGGAGATCGAATCCTGCCAGGTGTACTTCACCTATGAC	360		
Sbjct 1194	TTCTTCCATCTGCCCAATGCCTTGGAGATCGAATCCTGCCAGGTGTACTTCACCTATGAC	1253		
Query 361	CCCTGTGTGGAAGAGGAGGTGGAGGAGGATGGGTCAAGGCTGCCGAGGGATCTCCCCAC	420		
Sbjct 1254	CCCTGTGTGGAAGAGGAGGTGGAGGAGGATGGGTCAAGGCTGCCGAGGGATCTCCCCAC	1313		
Query 421	CCACCTCTGCTGCCTCTGGCTGGAGAACAGGATGACTACTGTGCCTTCCCGCCAGGGAT	480		
Sbjct 1314	CCACCTCTGCTGCCTCTGGCTGGAGAACAGGATGACTACTGTGCCTTCCCGCCAGGGAT	1373		

Tgfb β 1 cytoplasmic domain sequence

Score	Expect	Identities	Gaps	Strand
1973 bits(1068)	0.0	1068/1068(100%)	0/1068(0%)	Plus/Plus
Query 7		TGCCATAACCGCACTGTCATTACCACCGTGTGCCAAATGAAGAGGATCCATCACTAGAT		66
Sbjct 664		TGCCATAACCGCACTGTCATTACCACCGTGTGCCAAATGAAGAGGATCCATCACTAGAT		723
Query 67		CGCCCTTTTCATTTAGAGGGCACCACCTTAAAGATTAAATTTATGATATGACAACATCA		126
Sbjct 724		CGCCCTTTTCATTTAGAGGGCACCACCTTAAAGATTAAATTTATGATATGACAACATCA		783
Query 127		GGGTCTGGATCAGGTTTACCCTGCTTGTTCAAAGAACAATTGCCAGGACCATTGTGTTA		186
Sbjct 784		GGGTCTGGATCAGGTTTACCCTGCTTGTTCAAAGAACAATTGCCAGGACCATTGTGTTA		843
Query 187		CAAGAAAGCATTGGCAAAGGTCGGTTTGGAGAAGTTTGGCGAGGCAAATGGCGGGGAGAA		246
Sbjct 844		CAAGAAAGCATTGGCAAAGGTCGGTTTGGAGAAGTTTGGCGAGGCAAATGGCGGGGAGAA		903
Query 247		GAAGTTGCTGTGAAGATATTCTTCTAGAGAAGAGCGTTCATGGTTCCGAGAGGCAGAG		306
Sbjct 904		GAAGTTGCTGTGAAGATATTCTTCTAGAGAAGAGCGTTCATGGTTCCGAGAGGCAGAG		963
Query 307		ATTTATCAGACTGTAATGTTACGCCATGAAAATATCCTGGGATTTATAGCAGCAGACAAC		366
Sbjct 964		ATTTATCAGACTGTAATGTTACGCCATGAAAATATCCTGGGATTTATAGCAGCAGACAAC		1023
Query 367		AAAGACAATGGGACATGGACGCAGCTGTGGTTGGTGTGAGATTATCATGAGCATGGATCC		426
Sbjct 1024		AAAGACAATGGGACATGGACGCAGCTGTGGTTGGTGTGAGATTATCATGAGCATGGATCC		1083

Cd247 signaling domain sequence

Score	Expect	Identities	Gaps	Strand
632 bits(342)	5e-177	342/342(100%)	0/342(0%)	Plus/Plus
Query 1		AGAGCAAAATTCAGCAGGAGTGCAGAGACTGCTGCCAACCTGCAGGACCCCAACAGCTC		60
Sbjct 302		AGAGCAAAATTCAGCAGGAGTGCAGAGACTGCTGCCAACCTGCAGGACCCCAACAGCTC		361
Query 61		TACAATGAGCTCAATCTAGGGCGAAGAGAGGAATATGACGTCTTGGAGAAGAAGCGGGCT		120
Sbjct 362		TACAATGAGCTCAATCTAGGGCGAAGAGAGGAATATGACGTCTTGGAGAAGAAGCGGGCT		421
Query 121		CGGGATCCAGAGATGGGAGGCAAAACAGCAGAGGAGGAGGAACCCCAAGGAAGGCGTATAC		180
Sbjct 422		CGGGATCCAGAGATGGGAGGCAAAACAGCAGAGGAGGAGGAACCCCAAGGAAGGCGTATAC		481
Query 181		AATGCACTGCAGAAAGACAAGATGGCAGAAGCCTACAGTGAGATCGGCACAAAAGGCGAG		240
Sbjct 482		AATGCACTGCAGAAAGACAAGATGGCAGAAGCCTACAGTGAGATCGGCACAAAAGGCGAG		541
Query 241		AGGCGGAGAGGCAAGGGGCACGATGGCCTTTACAGGGTCTCAGCACTGCCACCAAGGAC		300
Sbjct 542		AGGCGGAGAGGCAAGGGGCACGATGGCCTTTACAGGGTCTCAGCACTGCCACCAAGGAC		601
Query 301		ACCTATGATGCCCTGCATATGCAGACCTGGCCCTTCGCTAA	342	
Sbjct 602		ACCTATGATGCCCTGCATATGCAGACCTGGCCCTTCGCTAA	643	

Figure 3. Sequence verification of CAR construct (A) DNA digestion with restriction endonuclease treatment. Samples – uncut lentiviral vector, 1 cut vector with *EcoRI*, another 1 cut vector with *Not I*, 2 cuts vector with *EcoRI* and *Not I* was prepared and loaded. The first lane and the last lane represent the band of the marker. (B) Sequence match with each CAR domain. Sequence from extracellular region to intracellular region is shown to be 100% matching the originated regions.

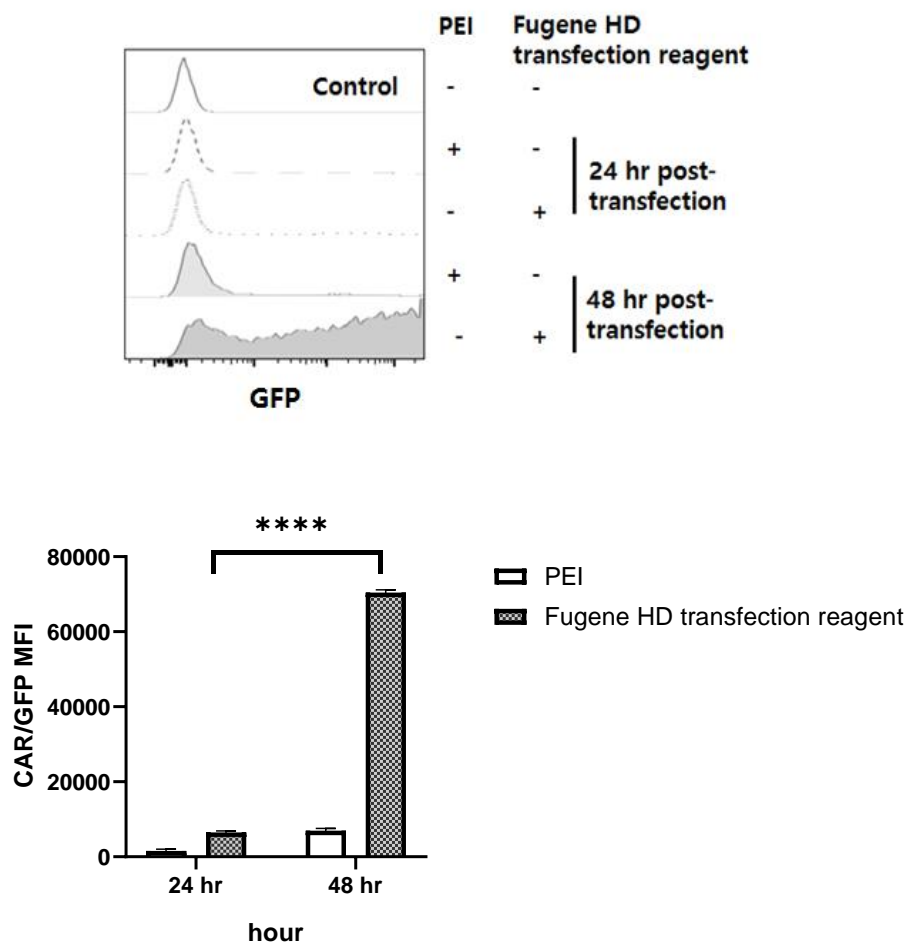
2) CAR expression verification in HEK293FT cell line

To test the activity of the lentiviral vector, transfection was done in HEK293FT cell line by two reagents called PEI and Fugene HD transfection reagent that utilize different transfection methods. And the reagent that showed better transfection efficiency was later used to produce lentivirus by co-transfecting packaging plasmids in HEK293FT cell line.

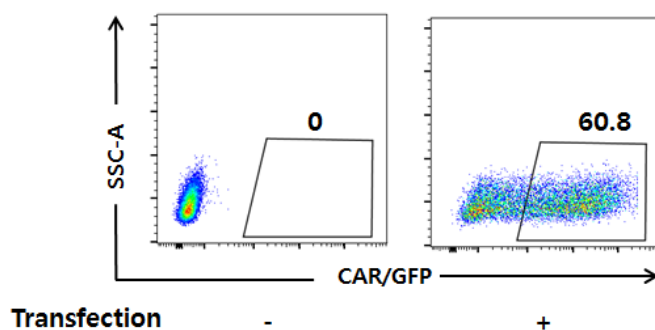
DNA can be introduced into a host cell by transfection with PEI, a stable cationic polymer, which condenses DNA into positively charged particles that bind to anionic cell surfaces, forming a liposome structure. DNA:PEI complex is then endocytosed by the cells, and the DNA is released into the cytoplasm (35). Fugene HD transfection reagent, on the other hand, uses a non-liposome system which is known to be less toxic to cells (36).

Interestingly, Fugene HD transfection reagent showed higher green fluorescence protein (GFP) mean fluorescence intensity (MFI), resulting in more than 4 times that of PEI 48 hr post-transfection (Fig. 4A). Green fluorescence was also observed from 24 hr post-transfection and identified using flow cytometry (Fig. 4B) and fluorescence microscope (Fig. 4C), once again proving the efficiency of using Fugene HD transfection reagent and the function of the lentiviral vector.

A



B



C

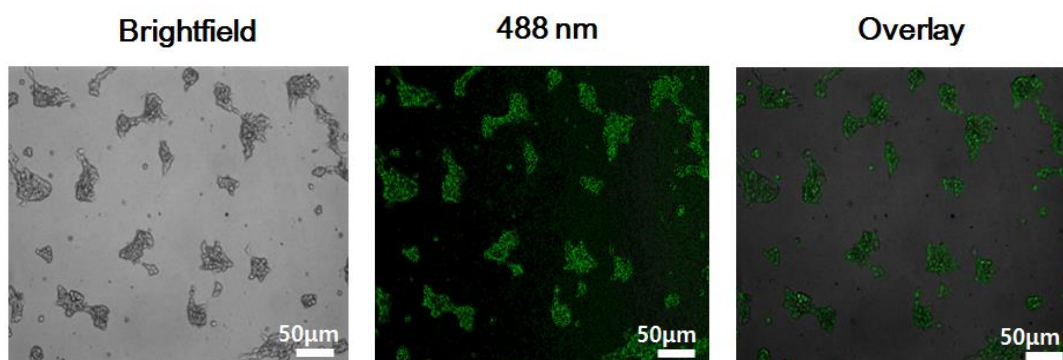


Figure 4. CAR expression in HEK293FT cell line (A) Comparison of transfection efficiency between reagents. Control sample was prepared by incubating HEK293FT cell line with Opti-MEM only. MFI was evaluated by Flowjo software. Error bars are SD, **** $p < 0.001$ determined by student's t -test. (B-C) GFP detection using Fugene HD transfection reagent in HEK293FT cell line by flow cytometry and fluorescence microscope using Zeiss fluorescence microscope in a $10\times$ lens. (A-C) All data are representative of 3 independent

experiments.

3. Generation of CAR–encoding lentivirus

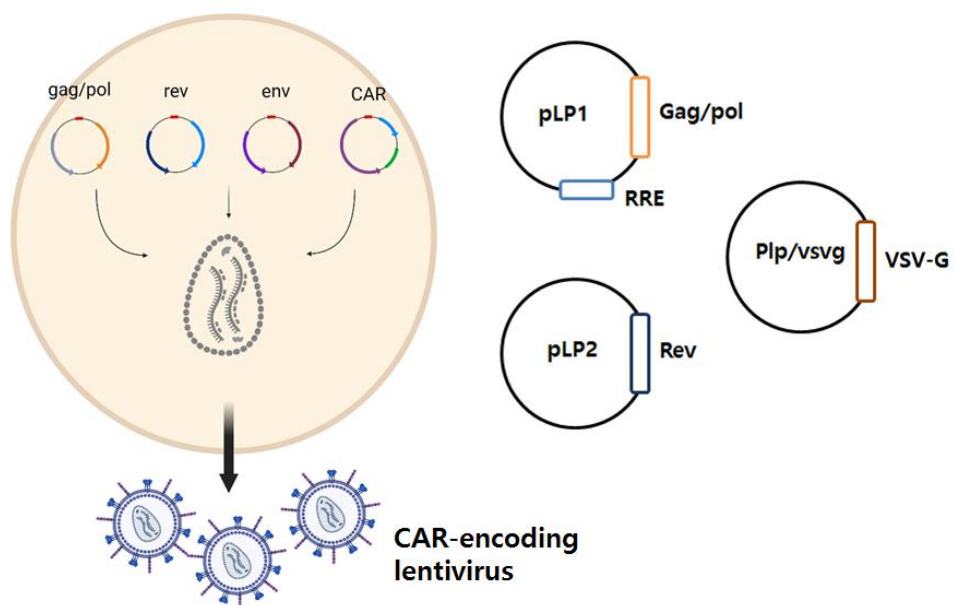
The method of generating lentivirus consists of two systems which are second and third–generation. In this study, third–generation system was utilized to produce CAR–encoding lentivirus, which required 4 plasmids – gag, pol, rev, and env possessing plasmids for making viral components and a transfer plasmid and a packaging cell line to wrap up the elements (37) (Fig. 5A). In detail, Gag, pol is a primary protein involved in packaging two copies of the viral genome for capsid retroviral core and used to encode enzymes essential for viral replication, such as reverse transcriptase, RNase H, and integrase. Rev regulates mRNA splicing and transportation to the cytoplasm and env provides the capsule of the virus. In this study, vesicular stomatitis virus g–protein (VSVG) was used due to its wide infectivity in receptor binding to host cells (38).

One day before transfection, HEK293FT cells (2.5×10^5 cells/mL) were plated in three 6–well plates, supplemented with complete media. The following day, media was changed to a complete media without antibiotic–antimycotic and geneticin 2 hr before co–transfection of lentivirus generating vectors. In a sterile 15 ml tube, Fugene HD transfection reagent was diluted at a ratio of 1:25 in a pre–warmed Opti–MEM (Gibco) and incubated for 5 min at room temperature. After incubation, plasmids of CAR, pLP1, pLP2, and pLP/VSVG were diluted in a 1: 1 : 1: 1 ratio based on their molecular

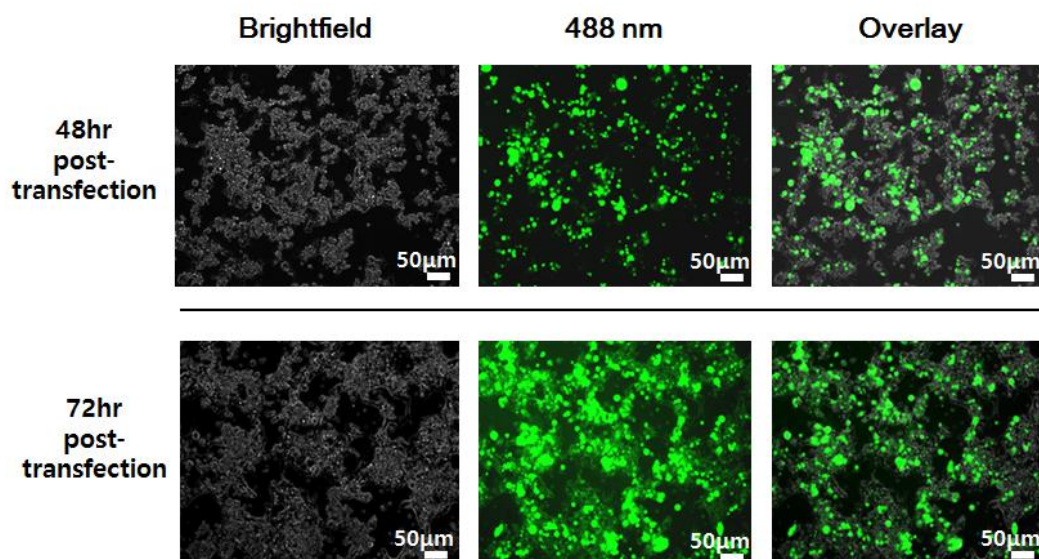
weight and incubated another 15 min at room temperature. DNA–Fugene HD transfection reagent complexes were added dropwise to each plate of cells and stored at 37° C in a 5% CO₂ incubator (IBC approval no. SNU IBC–20117–3). After 48 hr and 72 hr post–transfection, the viral supernatant was harvested and centrifuged at 500g for 10 min at 4° C to pellet cellular debris. Viral supernatant was filtered by 0.45 μ m polyethersulfone filter (Biofact) and concentrated by ultracentrifuge (Beckman Coulter, Brea, CA, USA) at 25000 rpm using SW28 rotor for 90 min, 4° C. Viral pellet was re–suspended in 1 \times Dulbecco's Phosphate–Buffer Saline (DPBS; Luscience, Hanam, Korea) and stored at 4° C for direct titration or –80° C for long–term use.

Fluorescence and morphology of co–transfected HEK293FT cell lines are shown 48 and 72 hr post–transfection (Fig. 5B). 72 hr, compared to 48 hr, expressed more green fluorescence excited by wavelength of 488 nm. Morphologically, co–transfected HEK293FT cell line developed syncytia, which is generally observed when lentivirus is produced (39) (Fig. 5C).

A



B



C

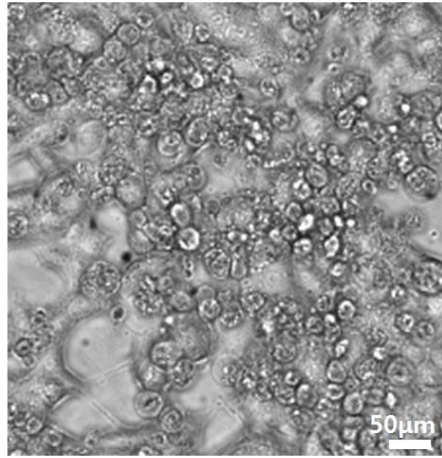


Figure 5. Production of CAR-encoding lentivirus (A) Visual scheme of how CAR-encoding lentivirus is packaged and produced. Illustration was created with "Biorender.com." (B) Microscopic image of fluorescence in HEK293FT cell line in 48 hr, 72 hr post co-transfection with Zeiss fluorescence microscope in 10 \times lens. (C) Development of syncytia in HEK293FT cell line 72 hr post co-transfection, detected by 10 \times lens with Zeiss fluorescence microscope. (B-C) Data are acquired from 5 independent experiments.

4. Titration of CAR–encoding lentivirus

Virus titration is roughly classified into structural and functional methods. The former incorporate sandwich enzyme–linked immunosorbent assay (ELISA) or quantitative reverse transcription–polymerase chain reaction (RT–qPCR), whereas the latter includes eGFP fluorescence detection by flow cytometry (40). In this study, both HIV–1 p24 ELISA and flow cytometry was done to examine the accurate titer. Structural titer was detected by HIV–1 p24 antigen ELISA (Zeptometrix, Buffalo, NY, USA). It works with viral supernatant that possesses p24 antigen, captured by p24 antibody coated on the plate. After the recapture of the anti–p24 biotinylated antibody, streptavidin–biotin amplifies the signal, and with the substrates added, the calculation of virus particle present in the viral supernatant is available.

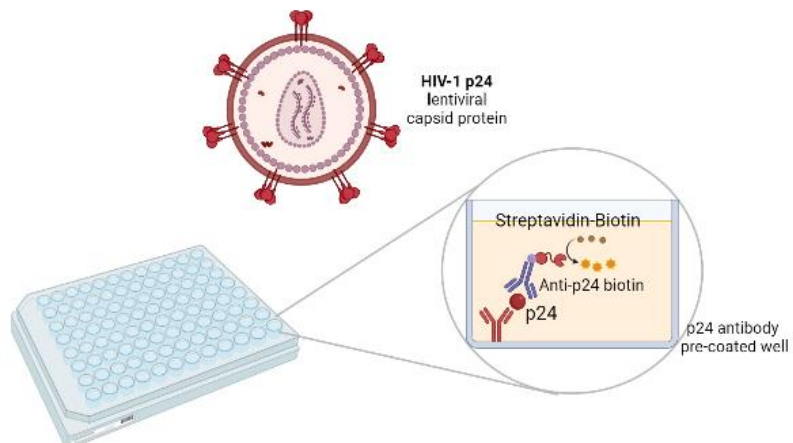
To measure functionally working viral particles, serial dilution was performed and analyzed by flow cytometry. Media containing concentrated virus and polybrene ($6 \mu\text{g/mL}$) – a cation that helps the transduction of virus into cells (41) – was prepared and diluted 1/10 sequentially, added in a plate seeded with 3×10^5 cells/well HEK293FT cell line, and incubated for 2 days (Fig 6A).

The standard curve of HIV–1 p24 antigen ELISA was drawn. Flow cytometry analysis proceeded with limiting dilution below, demonstrated the GFP⁺ population, showing dose–dependency in the

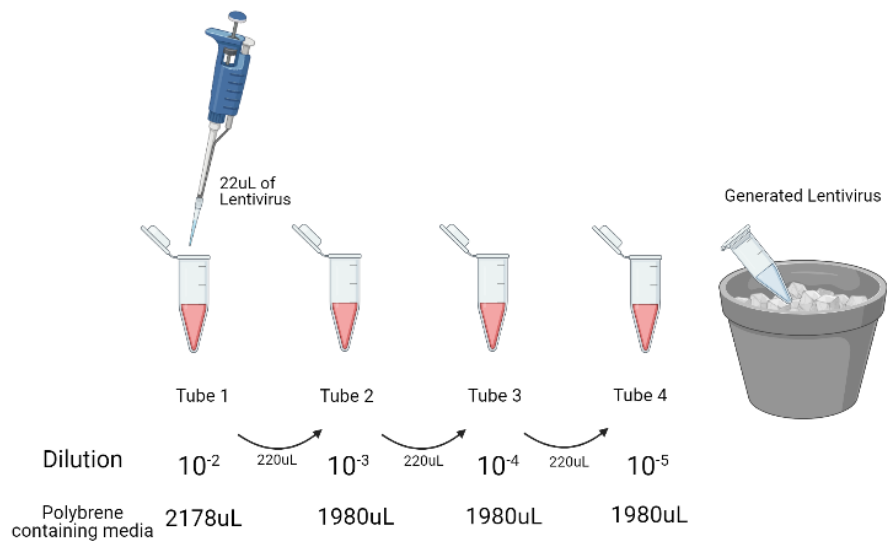
diluted ratios (Fig. 6B). Approximately 50% of GFP⁺ was shown in a dilution of 10⁻², 4% in 10⁻³, 0.3% in 10⁻⁴, and a much lower percentage in 10⁻⁵. When calculating the optimal viral titer, over 20% or less than 1% was ignored since the chance for each positive target cell to transduce twice increases significantly, resulting in an underestimation of the number of transducing particles. The functional titer was confirmed based on the chosen population and calculated in transduction units (TU)/mL.

Functional titer was twice lower than structural titer, implying that only half of the viral particles carry CAR with them. Even though it is still controversial on which strategy to use to calculate the accurate viral particle, in this study, the number of the viral particle was counted according to the functional titration done by flow cytometry and used for further experiments.

A



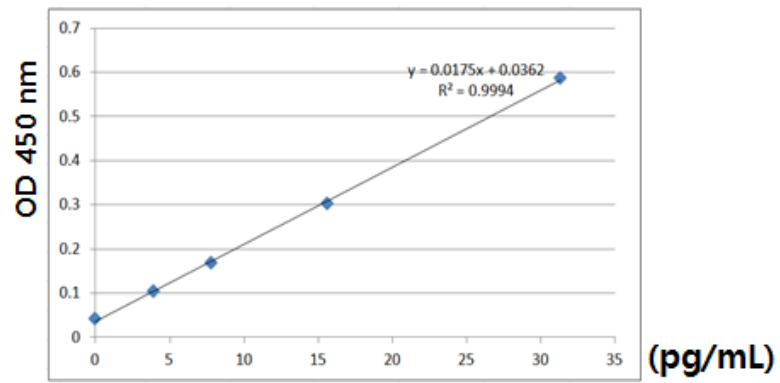
$$\frac{\text{OD-y intercept- blank}}{\text{Slope of the graph}} \times 100 \times \text{Dilution} = \text{__TU/mL}$$



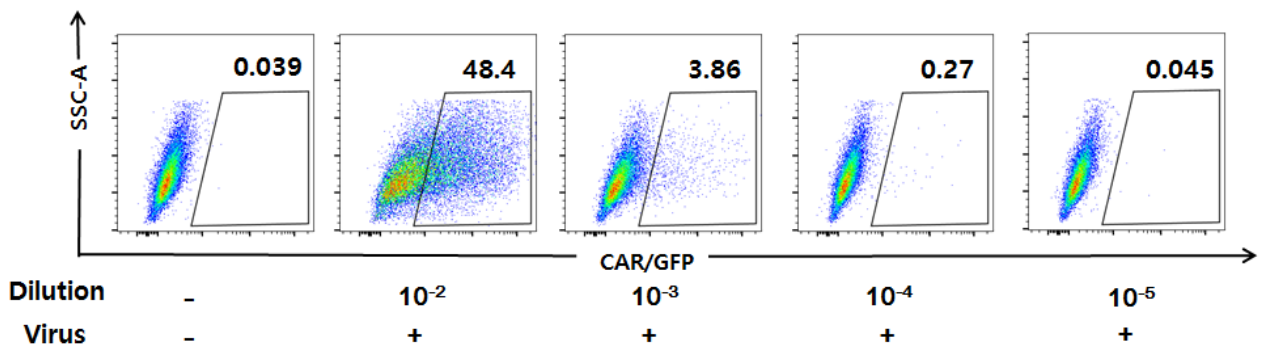
$$\frac{\text{Initial cell count} \times \text{GFP positive (\%)}}{\text{Dilution}} = \text{__TU/mL}$$

B

<ELISA Standard curve>



<Limiting Dilution Titration data>



C

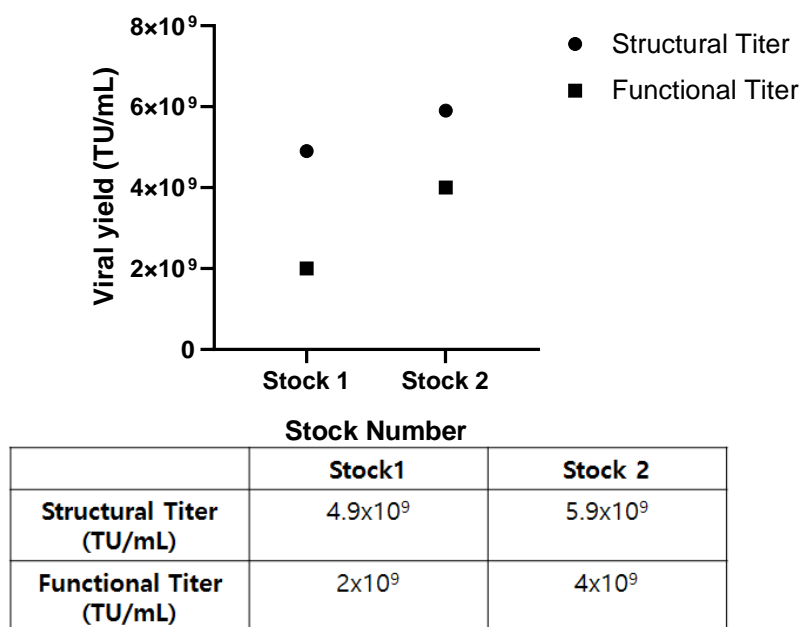


Figure 6. Calculation of CAR-encoding lentivirus particles (A) Experimental plan of HIV-1 p24 antigen ELISA and limiting dilution. Concentrated viruses were diluted $1/10^6$ in a complete media for ELISA and treated in a 96 well strip that contains p24 antibody. Below is a mathematical formula for calculating the number of viral particles. Samples were excited at a wavelength of 450 nm. The value of y-intercept and slope of the graph was applied from the standard curve of the ELISA graph. Underneath panel is a brief illustration of limiting dilution starting from 10^{-2} to 10^{-5} . The lower panel is the mathematical calculation for calculating virus particles from the result of flow cytometry. Initial cell count is the number of cells counted on the day of infection and GFP (%), meaning the positive population

observed by flow cytometry. Illustration was created with "Biorender.com." (B) Representative graph of HIV-1 p24 ELISA standard curve and flow cytometry transduction data of serial dilution. In the standard curve of ELISA, the R square value is 0.99, implicating the accuracy of the experiment. Gating was done based on the untransduced group. Titer was measured 48hr post-transduction. (C) Representative comparison graph and table showing structural and functional titer of CAR-encoding lentivirus. (B-C) Data are representative of 2 independent experiments.

5. CAR expression in mouse CD4⁺ T cells

1) Detection of the extracellular domain of CAR

In this study, naïve CD4⁺ T cells had to be enriched and transduced with CAR-encoding lentivirus. Based on many studies that high achievement of infection rate is generally reached 48 hr post-transduction (42), treatment of soluble CD40L (sCD40L) or co-culture with stimulated T cells were processed after that time point. To examine the expression of FoxP3, a critical transcriptional factor in Treg, detection by flow cytometry was done 4 days after co-culture with stimulated T cells because it is also studied that a high expression level of FoxP3 is seen after 4 days of stimulation in *in vitro* conditions (43) (Fig. 7A).

In mouse, naïve CD4⁺ T cell only comprises 5~10% of the splenocytes (43). In order to obtain enough cells, 3 mice were sacrificed per one independent test, which yielded about 7×10^7 to 2×10^8 splenocytes. Naïve CD4⁺ T cells were identified with markers such as CD45⁺CD3⁺CD4⁺CD25^{low}CD62L^{high}CD44^{low}. Naïve CD4⁺ T cells composed over 94% of the sorted cells suggesting that cells were well purified (Fig. 7B).

The binding process of a retrovirus to a cell is strongly influenced by the interaction between the envelope protein and the cellular receptor and many factors, such as temperature, pH, medium composition, and surface charge concentrations of viral particles and

cells. Among them, macromolecular cations are typically added to the medium during the retrovirus infection process of which increases transduction efficiency. The main effect of macromolecular cations so far known is that both the virus's surface and the cell's surface are negatively charged, and this electrostatic repulsive force is known to increase infection efficiency because macromolecular cation decreases (44–45).

Thus, many studies have suggested using multiple reagents such as polybrene(hexadimethrine bromide) and poly-L-lysine to facilitate the absorption of lentivirus to target cells (43). To compare which reagent to use, concentrated virus was treated into the sorted T cells in a multiplicity of infection (MOI) of 1 (Fig. 7C). Interestingly, the transduced population was over 10% different on average, much higher in polybrene-treated T cells. On the other hand, in cell death, data addressed no significant difference in treating polybrene and poly-L-lysine.

Before the direct application of polybrene to cells, adequate concentration had to be titrated, regarding its efficacy and toxicity (Fig. 7C middle panels). Treatment of polybrene with a concentration of 4 $\mu\text{g/mL}$ as a lowest, 6 $\mu\text{g/mL}$ as a medium, and 8 $\mu\text{g/mL}$ as a highest, revealed that 4 $\mu\text{g/mL}$ treated group showed the highest GFP⁺ percentage, approximately twice higher than 6 $\mu\text{g/mL}$ and 8 $\mu\text{g/mL}$. In addition, 8 $\mu\text{g/mL}$ rated the highest cell death, and the rest of 2 concentrations were non significantly different. Therefore in

this study, 4 $\mu\text{g/ml}$ polybrene was chosen as an optimal concentration for transducing mouse T cells.

Another critical factor that may enhance the viral infection is centrifugal inoculation, which is called spinoculation (46). Since spinoculation conditions can differ among many cell types, comparisons of transduction efficiency and toxicity were necessary. Data revealed a higher percentage of GFP(+) in spinoculated conditions, whereas no significant difference was suggested in cell death, which implies that spinoculation was adequate for this study (Fig. 7C right panels).

With these optimizations, naive CD4^+ T cells were treated with the concentrated lentivirus with 4 $\mu\text{g/mL}$ polybrene by centrifuging the cells at 700g for 120 min at 32° C. Then cells were transferred to a 37° C, 5% incubator for an overnight infection. The following day, media was changed to fresh T cell media and cultured for another one day to induce high expression of CAR.

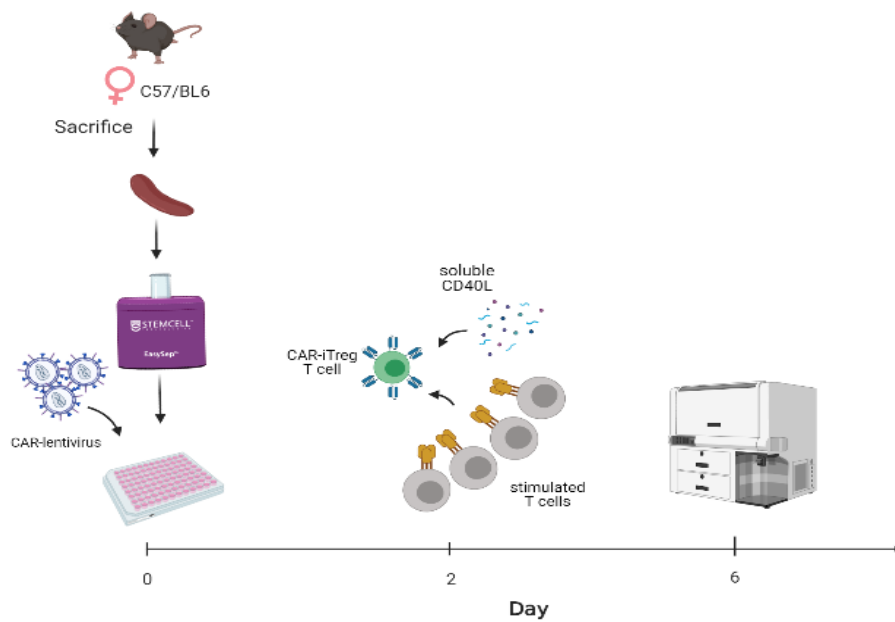
Several MOI were tested on sorted cells to check cell death and infection efficacy. Cells infected with MOI 10 and MOI 25 group expressed almost similar GFP^+ populations, however showing more apoptotic populations in MOI 25 group, addressing higher MOI might be deadly to cells due to cell stress it might provide (Fig. 7D).

After confirming CAR expression with GFP indirectly, it was essential that CAR exposes the extracellular domain, scFv properly. With no specific tag available for CAR-iTreg, sCD40L protein with

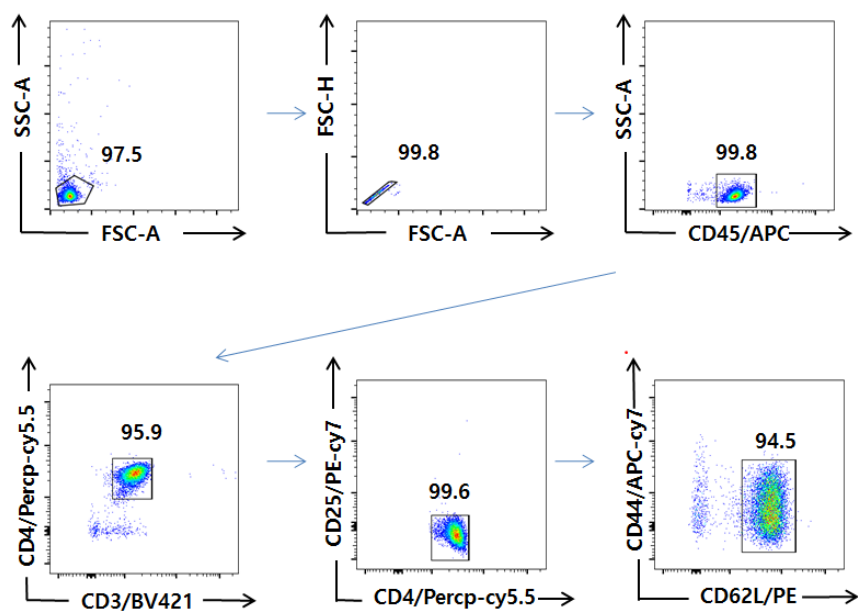
FLAG tag in the N-terminus was treated to prove its binding to CAR's scFv. Soluble CD40L protein (Enzo Life Sciences, Farmingdale, NY, USA) was treated in a concentration of 1 $\mu\text{g/mL}$ and incubated at 4° C for 1 hr.

Compared to naive CD4⁺ T cells treated with sCD40L alone, MOI 10 and MOI 25 groups showed about 64% and 80% in GFP⁺ FLAG⁺ positive populations. FLAG MFI also demonstrated a significant difference, approximately twice higher in MOI 25 than that of 10 group, addressing dose-dependency in MOI value. Also, following the treatment on different concentrations of sCD40L, starting from 1 $\mu\text{g/mL}$ to 5 $\mu\text{g/mL}$, MOI 10 group showed dose-dependency (29% vs 66.8% respectively), once again proving the expression of scFv (Fig 7E).

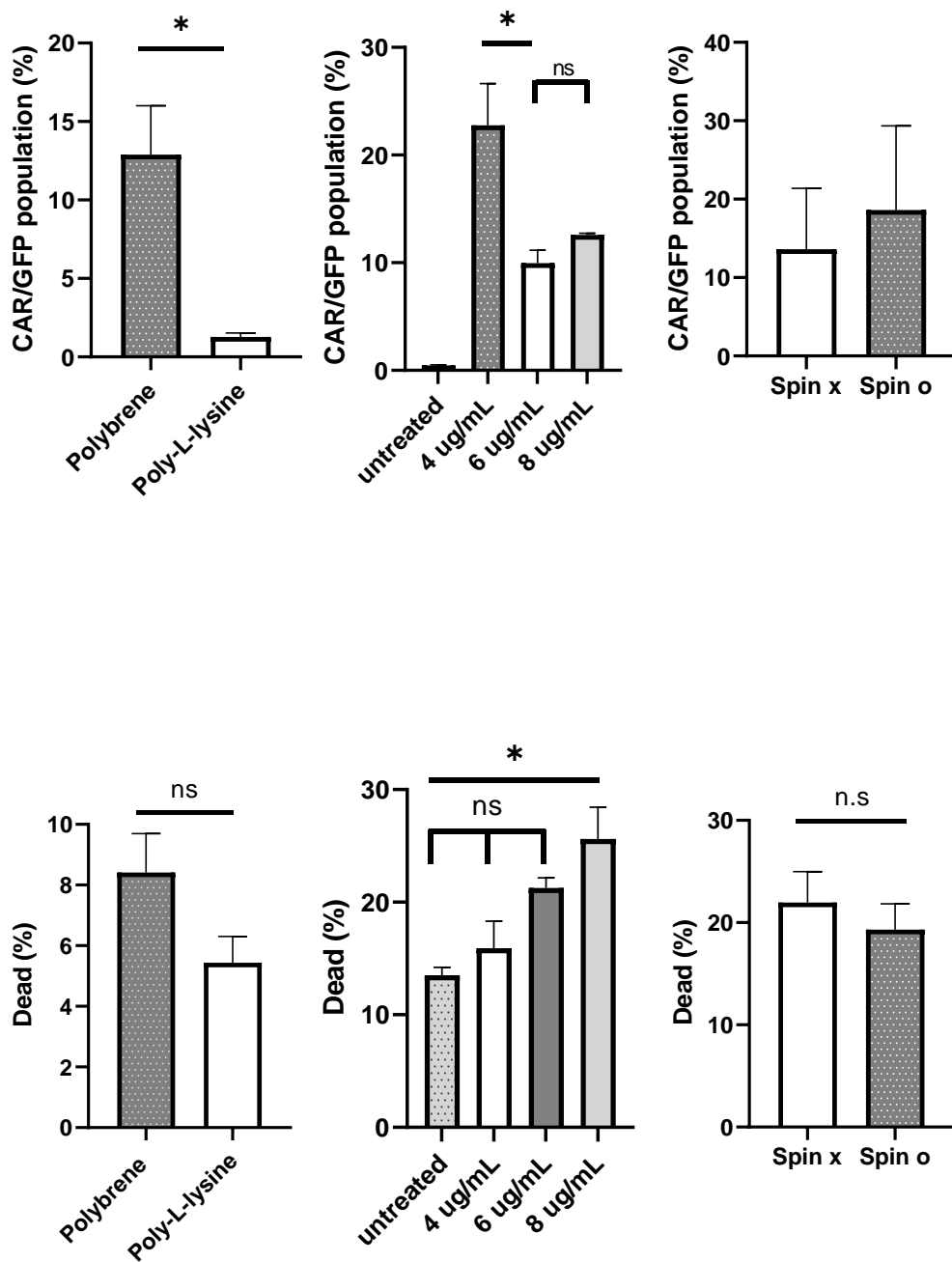
A



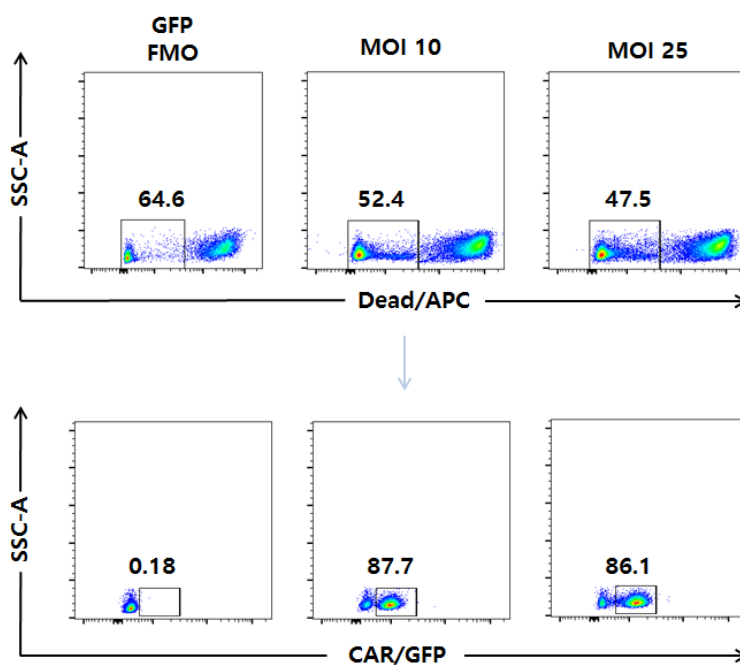
B



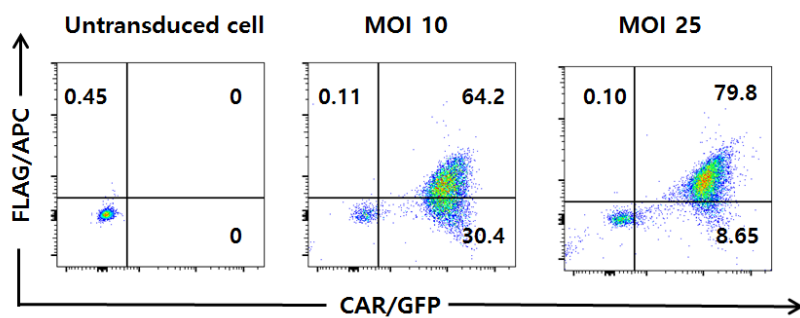
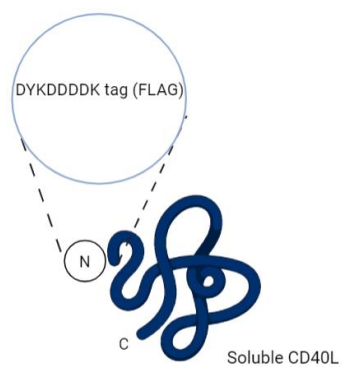
C



D



E



sCD40L	-	+	+	+
Transduction	+	+	+	+
APC stain	-	-	+	+
			(1ug/mL)	(5ug/mL)

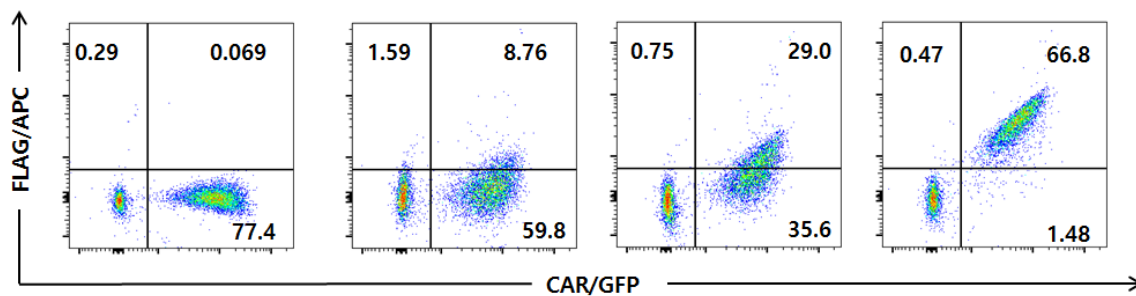


Figure 7. Extracellular expression of transduced CAR-T cells (A) Visual scheme of experimental design in confirming induction of CAR-iTreg. Illustration was created with "Biorender.com." (B) Gating strategy for naïve CD4⁺ T cells. To ensure the purity of naïve CD4⁺ T cells, lymphocytes were gated with CD45. Among CD45⁺ populations, CD3⁺CD4⁺ population was gated. CD25 negativity was added to exclude Tregs, leaving CD62L^{high} CD44^{low} population, identifying them as naïve CD4⁺ T cells. (C) Comparison of the transduced populations regarding the efficacy of transduction reagent and its toxicity along with the effect of spinoculation. Analysis was proceeded 2 days after transduction. ANOVA test was used, mean ± SD, **p* < 0.05, ns; non-significant. (D) Flow cytometry data of different infection rates with different MOI. The gating strategy was established based on GFP fluorescence minus one (FMO). (E) Visual illustration of sCD40L protein and flow cytometry data of sCD40L protein binding to CAR. The drawing was created with "Biorender.com." Data are representative of 3 (C, D) and 5 (B, E) independent experiments.

2) Detection of intracellular transcription factor Foxp3

Based on the timeline discussed in Fig 7A, cells were cultured for additional 4 days to detect intracellular transcription factor FoxP3 while feeding them with CD40L antigens either presented by soluble proteins or antigen-presenting cells (APCs).

In order to figure out the effect on transduced CAR-T cells, sCD40L (1 μ g/mL) was treated to cells and incubated for 4 days. MOI 25 group showed 16.3% of the GFP⁺FoxP3⁺ populations. Furthermore, overlaid histogram also demonstrated higher MFI of FoxP3 in the transduced CAR-T cells compared to that of untransduced cells (Fig. 8A).

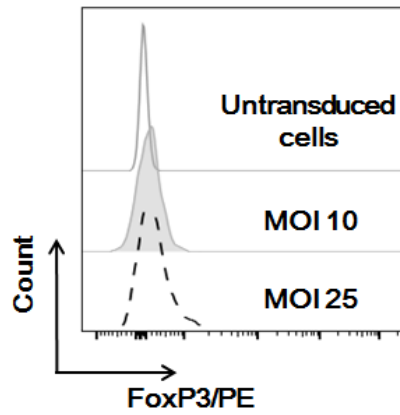
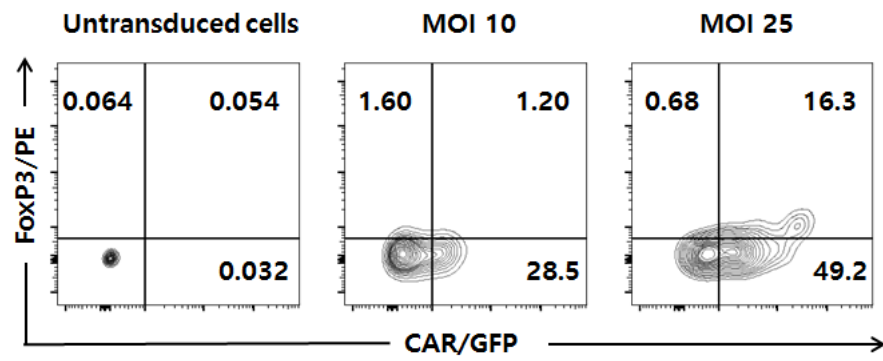
To mimic the *in vivo* environment in mice, CD3⁺ T cells were sorted out, stimulated, and co-cultured with transduced CAR-T cells. Mouse CD3⁺ T cells were negatively sorted out from splenocytes using mojosort CD3⁺ T cell isolation kit (BioLegend) and stained with anti-CD45, CD3 antibodies. Purity was over 95%, an average percentage of more than 3 independent studies (Fig. 8B).

Previous studies have shown that CD40L is detectable in T cells after 4–6 hours of stimulation and gradually decreases within 24 hours (42). To be provided as feeder cells for transduced CAR-T cells, the elevated expression level of CD40L was checked at 4, 6, 8, 24, 48 hr post-stimulation. CD3⁺ T cells were stimulated with plate-bound anti-CD3 (5 μ g/mL; 145–2C11) and anti-CD28 (5 μ g/mL;

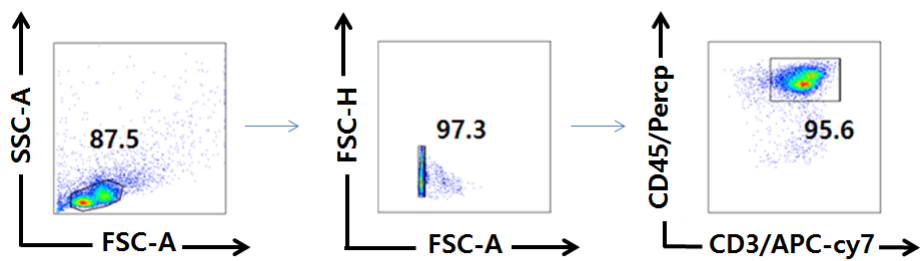
D665) antibodies, all from Invitrogen. After 5 to 6 hr stimulation, T cells were collected and centrifuged at 500g, 5 min. They were stained with fluorescence conjugated anti-CD40L antibody to certify the peak expression of CD40L molecule at the stated hours (Fig. 8C). There were no significant differences in the MFI of CD40L between 4, 6, 8 hr but stimulated T cells showed 2 times higher MFI of CD40L than unstimulated T cells (Fig. 8C). Thus, any stimulated T cells ranging from 4 hr to 8 hr were used to serve as APCs.

To further examine the effect of CD40L presentation, stimulated T cells were co-cultured at a ratio of 4:1 in a 96-well plate where transduced CAR-T cells were seeded. The result showed that MOI 10 and MOI 25 groups both expressed GFP⁺FoxP3⁺ population. And in detail, among cells in MOI 10 and MOI 25, GFP⁺ cells were estimated to be 6% and 5% respectively. Among GFP⁺ cells, about 50% and 40% showed FoxP3 positivity. To confirm that CAR-iTregs also express other Treg's functional markers, CTLA-4 and CD25 were stained. The result suggested that MOI 10 and 25 groups expressed similar expression of CTLA-4⁺CD25⁺ population with control FoxP3⁺ Tregs, confirming transduced CAR-T cells possess the traits that natural iTregs have (Fig. 8D).

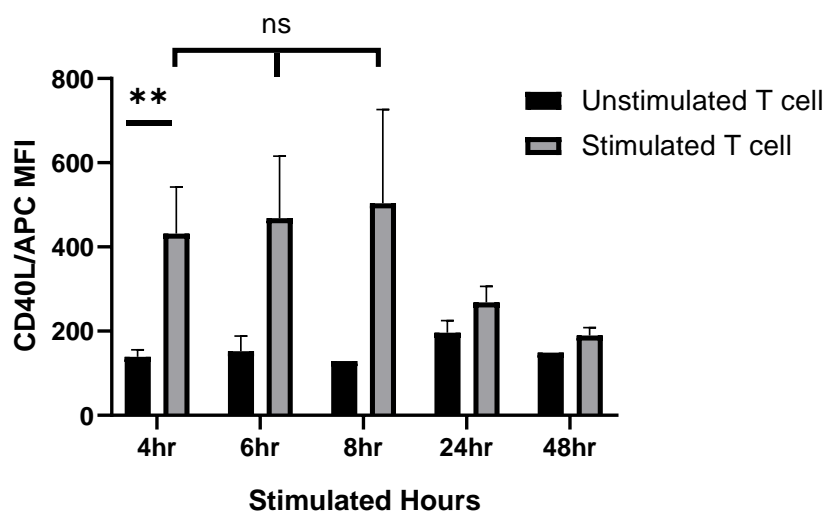
A



B



C



D

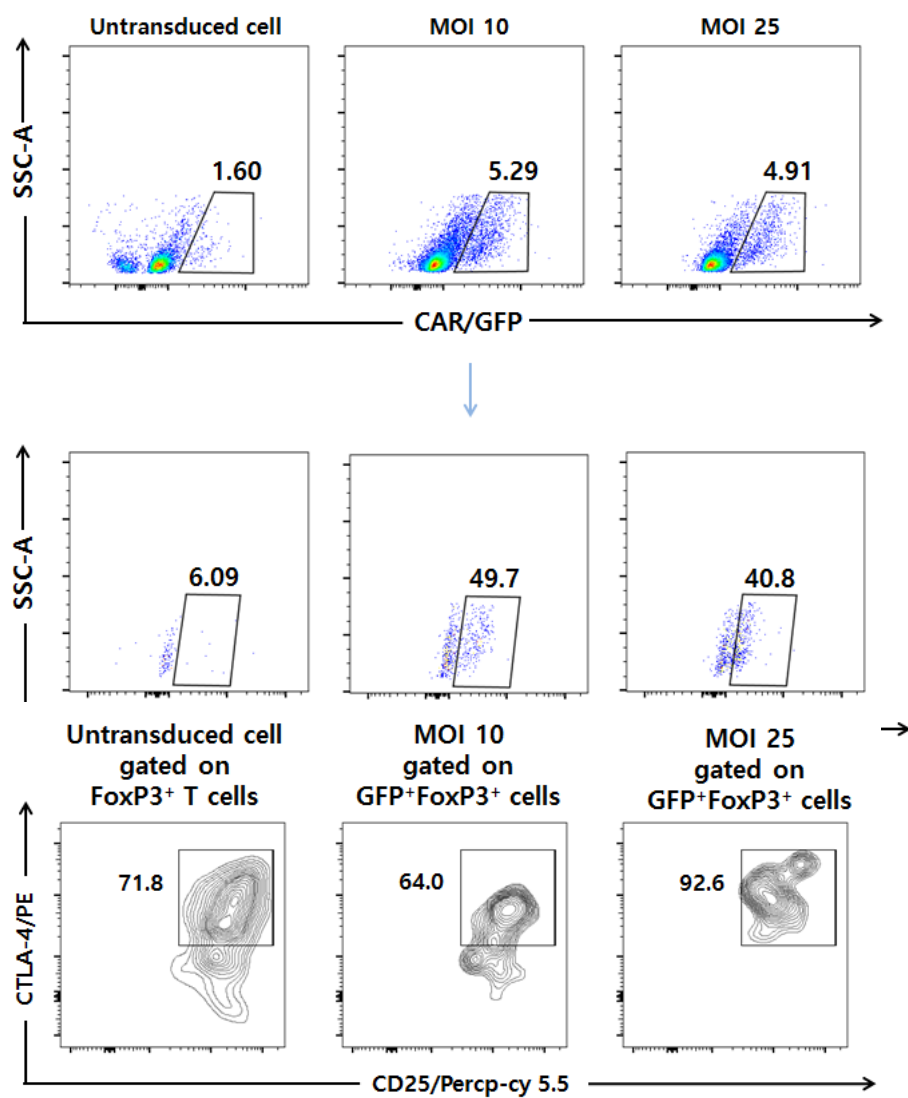


Figure 8. Induction of Foxp3 expression in transduced CAR-T cells

(A) Flow cytometry data of GFP⁺FoxP3⁺ population percentage in a soluble CD40L treated condition for 4-day incubation. The bottom panel is the comparison of a histogram of FoxP3 MFI among untransduced and transduced cells by different MOI. (B) Gating strategy of CD3⁺ T cells. Lymphocytes were gated with CD45. Among CD45⁺ populations, CD3⁺ populations were gated and identified as CD3⁺ T cells. (C) MFI of CD40L in activated T cells in different hours. Analysis was done with ANOVA test, mean \pm SD, ** p < 0.05, ns; non-significant. (D) Flow cytometry data of GFP⁺FoxP3⁺ populations in various MOI, co-cultured with stimulated T cells for 4 days. Gating of GFP and FoxP3 was based on untransduced cells. The lowest panel represents flow cytometry data of staining surface markers of Tregs. Gating of CTLA-4 and CD25 was based on FoxP3⁺ Tregs. Data are representative of 3 (A, D) and 5 (B, C) independent experiments.

DISCUSSION

The adoptive transfer of antigen-specific Tregs has been expected to be a promising therapeutic method for autoimmune diseases, severe allergy, and preventing graft rejection in organ transplantation. However, effective therapy has yet been established because of the difficulty in the process of isolation and proliferation in applying to actual clinical practice. Though recently, CAR showed their excellence in curing B cell malignancy by targeting CD19, CAR has not been widely developed in autoimmune and transplantation fields, with only a few CAR being generated.

CAR-iTreg construct, unlike conventional CD19-targeting CAR, suggests its specialty in inducing Treg cells through signaling, and in targeting of effector T cells *in vivo*, expected to relieve over-activation of effector T cells providing alluring immunotherapy in treating autoimmunity and graft rejection in transplantation.

Here, I brought a new approach in generating potent antigen-specific Tregs, using a CAR targeting CD40L. CAR-iTreg construct is novel in the term that it has *Il2rb* and *Tgfbr1* signaling domains added to the second conventional generation of CAR. These two domains gave CAR the capability to convert naïve CD4⁺ T cells into iTreg cells when stimulated with a specific antigen, CD40L.

CAR-iTreg is designed to use JAKs and STAT pathways for its

signaling. JAK/STAT pathway is known to convey information from signals outside of the cell to the cell nucleus, which controls the transcription of genes. To induce JAK-STAT pathway activation in CAR-iTregs in an antigen-dependent manner, first I incorporated a full-length cytoplasmic domain of *Il2rb* between the cytoplasmic domains of *Cd28* and *Cd247*. IL-2R has a γ chain associated with JAK3, which phosphorylates key tyrosines on the tail of the receptor and recruits an adaptor protein, facilitating gene regulation by STAT5 (47).

Then signaling domain of *Tgfb β 1* was added to include a TGF- β integrated signal to facilitate the differentiation into iTreg. With the use of TGF- β R1, it can transmit downstream signaling using SMAD2 and SMAD3, proteins that are renowned for cell proliferation, apoptosis, and differentiation (48).

Utilizing these concepts, CAR construct was inserted into a lentiviral vector along with a bicistronic construct of Zsgreen1 inside, making CAR detectable with green fluorescence. Lentivirus was generated to improve the efficacy in transducing mouse primary T cells. Harvested lentivirus was titrated and optimal MOI was set by treating various volumes of lentivirus to naïve CD4⁺ T cells. After feeding CD40L to transduced CAR-T cells, FoxP3 was detected, suggesting CAR-iTregs exhibit one of the representative characteristics of Treg cells. In this study, expansion of naïve CD4⁺ CAR-T cells by anti-CD3, anti-CD28 was unperformed, because

CAR itself bears CD3 and CD28.

However, there lie some limitations and improvements to be made. First of all, there were difficulties in gaining naïve CD4⁺ T cells, since the number of cells I could enrich was very limited. To adapt CAR-iTregs *in vivo*, obtaining a high yield of naïve CD4⁺ T cells from a patient would be necessary. Moreover, since stimulation is absent in my study, many cells went through apoptosis, making it more difficult to produce accurate data. Additionally, there were some batch effects in the GFP consistency in transduced cells. To remove this inconsistency, optimizing the methods in producing a stable virus or setting a stable transduction condition is necessary.

Besides, several issues are to be considered for further improvement on targeting, efficacy, and understanding the *in vivo* distribution and the fate of CAR-T cells. Ultimately, to extend the potential of CAR-T cell immunotherapy, CAR T-cells must possess specificity to the key antigens for a specific target. Even though CAR-iTreg is antigen-specific, more precise targeting can be achievable by aiming for additional specific antigens using bispecific CARs (49).

Also, the widespread application of CAR-T cells is uncertain due to its difficulty in expanding T cells on a large scale *ex vivo*. Long-term preparation is required to prepare CAR-T cells, including choosing autologous T cells and modification before reintroducing them into the patient. This slow process is not suitable for many

patients that do not allow a delay for cell manipulation and expansion of CAR-T cells.

There also lie new challenges regarding toxicity, which could bring side effects such as cytokine release syndrome (CRS) which is thought to be a result of the secretion of IL-6 (50). Nevertheless, until now, the risk factor of CRS is not fully understood.

Finally, the exhaustion of CAR may be problematic. Even though there had been many developments in generating various generations regarding CAR-T cells' longevity, the problem has not been unraveled. To ameliorate T cell exhaustion and improve CAR-T persistence some researchers suggest that CD137 costimulation, but not CD28 (51). However, it is still controversial among scientists, and further detailed analysis is needed.

REFERENCES

- 1) Zhang X, Olsen N, Zheng SG. The progress and prospect of regulatory T cells in autoimmune diseases. *J Autoimmun.* 2020;111:102461.
- 2) Sakaguchi S, Wing K, Yamaguchi T. Dynamics of peripheral tolerance and immune regulation mediated by Treg. *Eur J Immunol.* 2009;39(9):2331–6.
- 3) Nishizuka Y, Sakakura T. Thymus and reproduction: sex-linked dysgenesis of the gonad after neonatal thymectomy in mice. *Science.* 1969;166:753–5.
- 4) Sakaguchi S, Sakaguchi N, Asano M et al. Immunologic self-tolerance maintained by activated T cells expressing IL-2 receptor alpha-chains (CD25). Breakdown of a single mechanism of self-tolerance causes various autoimmune diseases. *J Immunol.* 1995;155(3):1151–64.
- 5) Thornton AM, Korty PE, Tran DQ et al. Expression of Helios, an Ikaros transcription factor family member, differentiates thymic-derived from peripherally induced FoxP3⁺ T regulatory cells. *J Immunol.* 2010;184(7):3433–41.
- 6) Shevyrev D, Tereshchenko V. Treg heterogeneity, function, and homeostasis. *Front Immunol.* 2020;10:3100.
- 7) Zheong S, Wang J, Wang P et al. IL-2 is essential for TGF- β to convert naïve CD4⁺CD25⁻ cells to CD25⁺Foxp3⁺ regulatory T cells

- and for expansion of these cells. *J Immunol.* 2007;178(4):2018–27.
- 8) Malek T, Castro I. Interleukin–2 receptor signaling: At the interface between tolerance and immunity. *Immunity.* 2010;33(2):153–165.
- 9) Burchill MA, Yang J, Vogtenhuber C et al. IL–2 receptor beta–dependent STAT5 activation is required for the development of Foxp3⁺ regulatory T cells. *J Immunol.* 2007;178(1):280–90.
- 10) Takimoto T, Wakabayashi Y, Sekiya T et al. Smad2 and smad3 are redundantly essential for the TGF–beta–mediated regulation of regulatory T plasticity and Th1 development. *J Immunol.* 2010;185(2):842–55.
- 11) Chen W, Jin W, Hardegen N et al. Conversion of peripheral CD4⁺CD25[–] naïve T cells to CD4⁺CD25⁺ regulatory T cells by TGF–beta induction of transcription factor Foxp3. *J Exp Med.* 2003;198(12):1875–86.
- 12) Kim H, Kim B, Letterio J et al. Smad–dependent cooperative regulation of interleukin–2 receptor α chain gene expression by T cell receptor and TGF– β . *J Biol Chem.* 2005;280:34042–47.
- 13) Zheng S, Wang H, Gray J et al. Natural and induced CD4⁺CD25⁺ cells educate CD4⁺CD25[–] cells to develop suppressive activity: the role of IL–2, TGF– β , and IL–10. *J Immunol.* 2004;172:5123–21.
- 14) Fu S, Zhang A, Yopp C et al. TGF– β induces Foxp3⁺T–regulatory cells from CD4⁺CD25[–] precursors. *Am J Transplant.* 2004;4:1614–27.

- 15) Elgueta R, Benson MJ, de Vries VC et al. Molecular mechanism and function of CD40/CD40L engagement in the immune system. *Immunol Rev.* 2009;229(1):152–172
- 16) Banchereau J, Dubois B, Fayette J et al. Functional CD40 antigen on B cells, dendritic cells, fibroblasts. *Adv Exp Med Biol.* 1995;378:79–83.
- 17) Bourgeois C, Rocha B, Tanchot C. A role for CD40 expression on CD8⁺ T cells in the generation of CD8⁺ T cell memory. *Science.* 2002;297(5589):2060–3.
- 18) van Kooten C, Banchereau J. Functions of CD40 on B cells, dendritic cells and other cells. *Curr Opin Immunol.* 1997;9(3):330–7.
- 19) Mazzei GJ, Edgerton MD, Losberger C et al. Recombinant soluble trimeric CD40 ligand is biologically active. *J Biol Chem.* 1995;270(13):7025–8.
- 20) Lai JH, Luo SF, Ho LJ. Targeting the CD40–CD154 signaling pathway for treatment of autoimmune arthritis. *Cells.* 2019;8(8):927.
- 21) Seijkens T, Kusters P, Engel D, et al. CD40–CD40L: linking pancreatic, adipose tissue and vascular inflammation in type 2 diabetes and its complications. *Diab Vasc Dis Res.* 2013;10(2):115–22.
- 22) Karnell JL, Rieder SA, Ettinger R et al. Targeting the CD40–CD40L pathway in autoimmune disease: Humoral immunity and beyond. *Advanced Drug Delivery Reviews.* 2019;141:92–103.
- 23) Neelapu SS, Tummala S, Kebriaei P et al. Chimeric antigen

receptor T– cell therapy–assessment and management of toxicities. *Nat Rev Clin Oncol.* 2018;15(1);47–62.

24) Chmielewski M, Hombach AA, Abken H. Antigen–specific T–cell activation independently of the MHC: Chimeric antigen receptor–redirected T cells. *Front Immunol.* 2013;4;371.

25) Sadelain M, Brentjens R, Riviere I. The basic principles of chimeric antigen receptor design. *Cancer Discov.* 2013;3(4):388–98.

26) Muller Y, Nguyen D, Ferreira L et al. The CD28–transmembrane domain mediates chimeric antigen receptor heterodimerization with CD28. *Front Immunol.* 2021;12;639818.

27) Dotti G, Gottschalk S, Savoldo B et al. Design and development of therapies using chimeric antigen receptor–expressing T cells. *Immunol Rev.* 2014;257(1):107–126.

28) Long AH, Haso WM, Shern JF et al. 4–1BB costimulation ameliorates T cell exhaustion induced by tonic signaling of chimeric antigen receptors. *Nat Med.* 2015;21(6):581–90.

29) Chmielewski M, Hombach A, Heuser C et al. T cell activation by antibody–like immunoreceptors: increase in affinity of the single–chain fragment domain above threshold does not increase T cell activation against antigen–positive target cells but decreases selectivity. *J. Immunol.* 2004;173(12): 7647–53.

30) Noyan F, Zimmermann K, Hardtke–Wolenski M et al. Prevention of allograft rejection by use of regulatory T cell with an MHC–specific chimeric antigen receptor. *Am J Transplant.*

2017;17(4):917–30.

31) Boardman DA, Philippeos C, Fruhwirth GO et al. Expression of a chimeric antigen receptor specific for donor HLA class I enhances the potency of human regulatory T cells in preventing human skin transplant rejection. *Am J Transplant*. 2017;17(4):931–43.

32) Southern PJ, Berg P. Transformation of mammalian cells to antibiotic resistance with a bacterial gene under control of the SV40 early region promoter. *J Mol Appl Genet*. 1982;1(4):327–41

33) Zheng S, Wang J, Horwitz D. Cutting edge: FoxP3⁺CD4⁺CD25⁺ regulatory T cells induced by IL-2 and TGF- β are resistant to Th17 conversion by IL-6. *J Immunol*. 2008;180(11):7112–6.

34) Gilliland L, Norris NA, Marquardt H et al. Rapid and reliable cloning of antibody variable regions and generation of recombinant single chain antibody fragments. *Tissue Antigens*, 1996;47(1):1–20.

35) Longo PA, Kavran JM, Kim MS et al. Transient mammalian cell transfection with polyethylenimine (PEI). *Methods Enzymol*. 2013;529:227–40.

36) Jacobsen L, Calvin S, Lobenhofer E. Transcriptional effects of transfection : the potential for misinterpretation of gene expression data generated from transiently transfected cells. *Biotech*. 2009;47(1):617–624.

37) Larson B, Pan D, Rickard M et al. Evaluation of second- and third generation lentiviral vector systems for integration and expression of alpha-L-Idronidase in Mucopolysaccharidosis Type I. *Mol Therapy*.

2002;5(5);supplement:S181.

38) Ci Y, Yang Y, Xu C et al. Vesicular stomatitis virus G protein transmembrane region is crucial for the hemi-fusion to full fusion transition. *Sci Rep.* 2018;8(1);10669

39) Bauler M, Roberts J, Wu C et al. Production of lentiviral vector using suspension cells grown in serum-free media. *Mol Ther.* 2019;17:58–68.

40) Geraerts M, Willems S, Baekelandt V et al. comparison of lentiviral vector titration methods. *BMC Biotechnol.* 2006;6:34

41) Gill KP, Denham M. Optimized transgene delivery using third-generation lentiviruses. *Curr protoc Mol Biol.* 2020;133(1):e125.

42) Manning JS, Hackett AJ, Darby NB Jr. Effect of polycations and on sensitivity of BALB/3T3 cells to murine leukemia and sarcoma virus infectivity. *Appl Microbiol.* 1971;22(6): 1162–3.

43) Flaherty S, Reynolds JM. Mouse naïve CD4⁺ T cell isolation and *in vitro* differentiation into T cell subsets. *J Vis Exp.* 2015;(98):52739.

44) Lee SG, Kim S, Robbins PD et al. Optimization of environmental factors for the production and handling of recombinant retrovirus. *Appl Microbiol.* 1996;45(4):477–483.

45) Denning W, Das S, Guo S et al. Optimization of the transductional efficiency of lentiviral vectors: effect of sera and polycations, *Mol Biotechnol.* 2013;53(3)308–14.

46) Yan R, Zhang Y, Cai D, Liu Y et al. spinoculation enhances HBV

infection in NTCP-reconstituted hepatocytes. *PLoS One*. 2015;10(6):e0129889.

47) Zhang Q, Nowak J, Vonderheid EC et al. Activation of Jak/STAT proteins involved in signal transduction pathway mediated by receptor for interleukin 2 in malignant T lymphocytes derived from cutaneous anaplastic large T-cell lymphoma and Sezary syndrome. *Proc Natl Acad Sci USA*. 1996;93(17):9148–53.

48) Derynck R, Zhang YE. Smad-dependent and smad-independent pathways in TGF- β family signaling. *Nature*. 2003;425:577–84.

49) Cronk RJ, Zurko J, Shah NN. Bispecific chimeric antigen receptor T cell therapy for B cell malignancies and multiple myeloma. *Cancers (Basel)*. 2020;12(9):2523.

50) Pabst T, Bacher U. Analysis of IL-6 serum levels and CAR T cells-specific digital PCR in the context of cytokine release syndrome. *Exp Hematol*. 2020;88:7014.e3.

51) Muller YD, Nguyen DP, Ferreira L et al. The CD28-transmembrane domain mediates chimeric antigen receptor heterodimerization with CD28. *Front Immunol*. 2021;12:639818.

국문 초록

서론: 조절 T 세포는 생체 내의 면역반응을 조절하고 자신의 항원에 대한 자가면역관용을 유지하는 역할을 수행한다. 최근에는 조절 T 세포를 주입하여 자가면역질환을 치료하는 동물 모델 연구가 진행되고 있다. 하지만, 조절 T 세포는 생체 내에 낮은 비율로 존재하므로 이를 실제 임상에 적용하기 위해 분리 및 증식시키는 과정에 어려움이 있다. 따라서 본 연구에서는 키메라항원수용체(CAR)를 이용하여 생체 내 조절 T 세포의 수를 늘리는 방안을 마련하고자 하였다. CAR-유도 조절 T 세포(iTreg)은 CD40L에 특이적인 단일쇄 가변 단편(scFv) 도메인을 가지고 있어, 활성화된 T세포가 발현하고 있는 CD40L와 만났을 때, 신호전달 도메인들에 의해서 미감작 T 세포가 조절 T 세포로 분화하게끔 디자인되었다.

방법: CAR 벡터의 발현을 확인하기 위해서 염기서열결정을 진행하였으며, HEK293FT 세포주에 형질전환을 하여 형광발현을 확인하였다. 바이러스의 입자의 수는 ELISA와 Flow cytometry로 계산하였다. MACS 시스템을 이용하여 분리한 마우스 미감작 CD4⁺ T 세포에 렌티 바이러스를 전이시켰다. 이후 발현된 CAR의 구조적, 기능적 측면을 확인하기 위해서 항체 염색을 통해 다양한 표현과 기능 마커의 검출을 수행하였다.

결과: CAR의 발현은 pLVX-IRES-ZsGreen1 벡터에 존재하는 ZsGreen (GFP) 형광으로 확인하였다. 마우스 미감작 CD4⁺ T 세포에 CAR가

전이된 상태의 세포 외 도메인의 발현은 수용성 CD40L 단백질이 scFv에 결합하는 것을 통해 확인하였다. 또한, 마우스의 활성화된 CD3⁺ T 세포와 함께 배양한 후, FoxP3 등을 발현하는 것을 확인하였다.

결론: 본 연구에서 고안된 CAR-iTreg은 활성화된 T 세포에 있는 CD40L를 표적하도록 디자인되었다. CD40L와 결합한 후, 전이된 미감작 CD4⁺ CAR-T 세포들이 유도 조절 T 세포의 대표적인 전사인자인 FoxP3와 표면 표지자를 발현하였기에, 자가면역질환의 치료 및 이식거부반응 억제에 치료제로 사용할 수 있는 실마리를 제공할 것으로 기대한다.

주요어 : 유도 조절 T 세포, 키메라항원수용체, CD40L, 자가면역질환, 장기이식

학번 : 2019-20372